Myocardial Differentiation is Dependent on Endocardial Signaling During Early Cardiogenesis *in vitro*

By

Leshana Saint-Jean

Dissertation

Submitted to the Faculty of the

Graduate School of Vanderbilt University

in partial fulfillment of the requirements

for the degree of

DOCTOR OF PHILOSOPHY

in

Cell and Developmental Biology

October 31, 2018

Nashville, Tennessee

Approved:

David Bader, Ph.D.

H. Scott Baldwin, M.D.

Christopher V. Wright, D.Phil.

Antonis Hatzopoulos, Ph.D., F.A.H.A.

Charles C. Hong, M.D., Ph.D.

ACKNOWLEDGEMENTS

I would like to thank the members of my committee for their scientific guidance, patience and funny banter throughout my Graduate career. I am also grateful for the wonderful past and present members of the Baldwin Laboratory who were always supportive and made me feel like part of the family. I would like to thank my graduate mentor, Scott Baldwin, for sharing his vast knowledge of the heart development field and for shepherding me towards becoming an independent researcher. In addition, I am appreciative of the friendships I developed with former and current members of the Goudy Lab and the Merryman Lab. I also want to acknowledge that the success of this project was due largely to the financial support provided by the National Heart, Lung, And Blood Institute of the National Institutes of Health, the American Heart Association Predoctoral Fellowship, and the Cellular, Biochemical, and Molecular Sciences Training Program. Lastly, I am extremely thankful for my husband and son, who have made my life an ongoing adventure.

TABLE OF CONTENTS

LIST OF FIGURES

LIST OF ABBREVIATIONS

β-gal	Beta-galactosidase
a	Atria
A	AscI
AVC	Atrioventricular canal
AVE	Anterior visceral endoderm
BAC	Bacterial artificial chromosome
Bmp	Bone morphogenic protein
CC	Cardiac cushion
CD31	CD31/Pecam-1
Cdh5	VE-cadherin
CHD	Congenital heart defect
CNC	Cardiac neural crest
cTnT	Cardiac troponin T
DAPI	4',6-diamidino-2-phenylindole
D_	Differentiation Day
DMEM	Dulbecco's modified eagle medium
DMSO	Dimethyl sulfoxide
DTR	Diphtheria toxin receptor
E_	Embryonic day
E1	Exon 1
E2	Exon 2
EB	Embryoid body
EC	Endocardial cell
ECM	Extracellular matrix
EDTA	Ethylene diamine tetraacetic acid
EGF	Epidermal growth factor
EMT	Epithelial-to-mesenchymal transition
ESC	Embryonic stem cell
ET	Endothelial cell
FACS	Fluorescence activated cell sorting
FBS	Fetal bovine serum
FGF	Fibroblast growth factor
FHF	First heart field
GFP	Green fluorescent protein
GREM2	GREMLIN 2
HBSS	Hank's balanced salt solution
hiPSCs	Human-induced pluripotent stem cells
IGF	Insulin-like growth factor
IMDM	Iscove's modified Dulbecco's medium
JNK	c-Jun N-terminal Kinase
LIF	Leukemia inhibitory factor
M	Molar
MHC	Myosin heavy chain
MLC	Myosin light chain
mM	Millimolar
NFATc1	Nuclear factor of activated T-cells
NICD	Notch intracellular domain

Nrg1	Neuregulin1
OFT	Outflow tract
P1	P1 promoter
P2	P2 promoter
PBS	Phosphate Buffered Saline
pBSKS	pBluescript KS+
PDGF	Platelet-derived growth factor
pHH3	Phosphohistone H3
PE	Proepicardium
qPCR	Quantitative real-time PCR
SHF	Secondary heart field
T	Brachyury
TGF	Transforming growth factor
μM	Micromolar
VEGF	Vascular endothelial growth factor
V	Ventricular lumen

CHAPTER I

THE ORIGIN AND DIVERSE ROLES OF THE ENDOCARDIUM DURING HEART DEVELOPMENT

A. Introduction

Congenital heart defect (CHD) is linked to nearly 1% of live births and is prevalent among major congenital deformities (van der Linde et al., 2011, Triedman et al., 2016). Though the life expectancy of those with CHD has increased due to successful surgeries and cutting-edge medical therapies, it remains the foremost cause of death. Therefore, it is essential that we continue efforts to broaden our understanding of normal heart development and cell biology and to delineate the underlying pathological molecular changes that cause CHD.

The heart is first the organ to form and function during mammalian development to supply necessary nutrients that support growth and development (Srivastava et al., 2006). Before the heart can accomplish such a goal, it must first endure multiple morphological changes that depend on cell-cell interactions. In the past, most of the studies regarding cell-cell interactions involved in heart development have centered on those between myocardial cells and derivatives of the endoderm and ectoderm. One example includes Neural-crest cells, which were found to invade the heart from the pharyngeal region and play a role in septation of the cardiac outflow tract (OFT) (Kirby et al., 1995, Srivastava et al., 1997, Hutson et al., 2003, Stoller et al., 2005, Brown et al., 2006). The endoderm has been reported to promote myocardial specification by signaling through multiple signaling pathways that include members of the fibroblast growth factor (FGF) and transforming growth factor beta (TGFβ) families (Abu-Issa et al., 2007). Cell-cell interactions that occur during heart development also include those between derivatives of the cardiac mesoderm, more specifically between endocardial and myocardial cells. Until recently most of the research regarding cardiogenesis has focused on the origin and development of the myocardium while failing to identify the various roles of the endocardium. It is now becoming quite evident that the endocardium is essential for establishing a functional, four-chambered heart.

B. The Origin of the Endocardium

The endocardium represents a separate, subpopulation of the endothelium located in the heart that develops during the initial stages of cardiac ontogeny. During this time in development, progenitors from the cardiac mesoderm that express Brachyury/T (*T*) ingress through the primitive streak and take up residence within the splanchnic mesoderm (Kouskoff et al., 2005). These cardiogenic precursors will eventually express *Flk1* and give rise to components of both the first and secondary heart fields (Motoike et al., 2003, Kouskoff et al., 2005, Ema et al., 2006, Kattman et al., 2006). The emergence of endocardial cells can be identified around this time of development by the expression of N-cadherin in the chick embryo during gastrulation (Linask et al., 1992). Between Hamburger and Hamilton (H&H) stages 6-8, the underlying endoderm signals to endocardial precursors located within the epithelium of the cardiac forming region to downregulate N-cadherin and undergo mesenchymal transformation before moving into the intermediate space between the developing myocardium and the anterior visceral endoderm (AVE) (Linask et al., 1992, Sugi et al., 2003).

Studies have suggested that the endocardium arise de novo from a subset of mesodermal precursors in a process that resembles endothelial cells during vasculogenesis (Harris et al., 2010). At stage 7 of development in quail embryos, endocardial precursors within the precardiac mesoderm express endothelial cell marker QH-1 (Sugi et al., 1996). At stage 8, the endocardial precursors form a branching network of vessels that consist of QH-1 positive cells outside of the cardiac region (Coffin et al., 1988, Sugi et al., 1996). During the lateral folding of the embryo along the ventral midline, the bilateral cardiac regions combine to form what is known as the heart tube. By stage 9 of development, QH-1 positive cells of the chord-like vessels within the plexus undergo remodeling and migrate to establish the inner, endocardial lining of the heart tube (HS. et al., 1996 , Sugi Y et al., 1996). A path by which blood can flow through the contracting heart into the vasculature system is then established by connecting the endocardium with the ventral aorta and the vitelline vein (Coffin et al., 1988, Coffin et al., 1991). A similar process of endocardiogenesis was reported in the mouse model (Baldwin et al., 1994).

C. Possible Sources of the Endocardium

Multipotent Cardiovascular Progenitor Cells

There are two schools of thought concerning the origin of endocardial cells. One model proposes that endocardial and myocardial cells arise from common multipotent progenitors located in the bilateral heart fields (Fig 1.1) (Motoike et al., 2003, Wu et al., 2006). This model is in support of results reported by Tam *et al.* that revealed single cells labeled within the posterior epiblast at the onset of gastrulation contributed to both endocardium and myocardium (Tam et al., 1997). Lineage tracing was also used in mice to demonstrate that *Flk1* expression, an early marker of hematopoietic and vascular progenitors, delineates various mesodermal progenitors such as those of the endocardium and myocardium (Ema et al., 2006). In addition, *in vitro* studies using mouse embryonic stem cells (mESCs) demonstrated that $T^+/Flk1^-$ mesodermal progenitors had the potential to produce a subsequent population of $Flk1^+$ mesodermal progenitors that differentiated into cardiomyocytes, vascular smooth muscle cells, and endothelial cells (Kattman et al., 2006, Christoforou et al., 2008). The QCE-6 cell line was established from the precardiac mesoderm of quail embryos and also demonstrated bi-potential capability. QCE-6 cells could differentiate into both endocardial and myocardial cells under certain conditions (Eisenberg et al., 1995a).

Recent studies suggest endocardial cells integrate into the heart during embryogenesis in two temporally separate stages. Milgrom *et al.* identified a field of endocardial progenitors in the chicken that was medial to the cardiac crescent and connected with the endothelial plexus (Milgrom-Hoffman et al., 2011). Anterolateral fusion of the cardiac crescent produced a primitive heart tube consisting of an outer lining of myocardial cells and an inner lining of endocardial cells that were all derived from the first heart field (FHF) (Zaffran et al., 2004). Further development and elongation of the heart tube along with looping occurred through proliferation and the contribution of cells from the secondary heart field (SHF) at the arterial and venous poles (Buckingham et al., 2005). Genetic fate mapping demonstrated that cells derived from the SHF gave rise to several cardiac lineages including endocardial cells and endocardial-

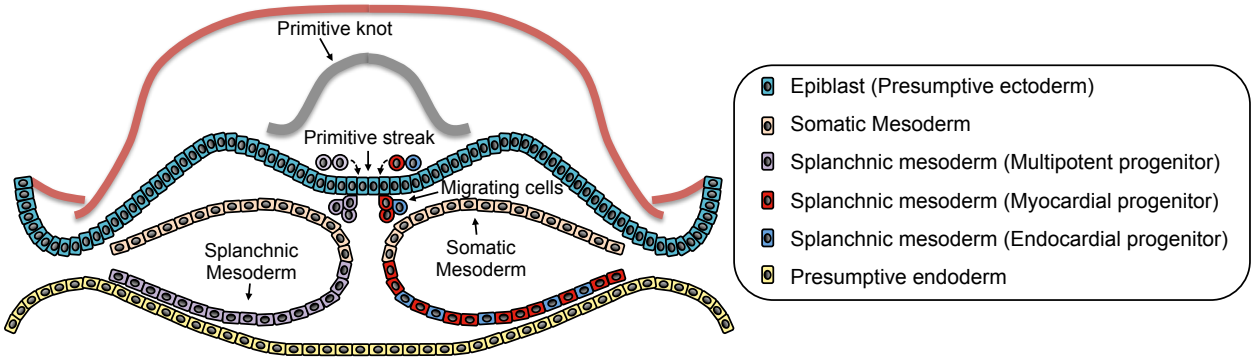

Figure 1.1 Origin of endocardial cells. One model regarding the origin of endocardial cells suggests they arise from common multipotent progenitors that differentiate after exiting the primitive streak during gastrulation and also gives rise to myocardial cells within the cardiac mesoderm. A second model of origin states that the myocardium and the endocardium are derived from two spatially segregated populations of progenitor cells. It is postulated that these progenitors exit the primitive streak during gastrulation and gather within the cardiac mesoderm prior to differentiating in close proximity and around the same time.

derived mesenchymal cells of the cushions (Moretti et al., 2006, Wu et al., 2006, Christoforou et al., 2008). Furthermore, Mice null for *Isl1*, a marker of the secondary heart field, lacked the right ventricle, the outflow tract, and most of the atria (Cai et al., 2003). Verzi *et al.* further demonstrated the dual potential of mesodermal derivatives within the SHF utilizing a *Mef2c* enhancer Cre line (Verzi et al., 2005).

Notwithstanding the distinct developmental potential of endocardial cells, their genetic profile is very similar to that of vascular endothelial cells (VECs), thus making it difficult to study them as individual populations. To address this quandary, Misfeldt *et al.* generated an *NFATc1-nuc-LacZ* BAC reporter transgenic mouse line which expresses β-galactosidase (β-gal) under the regulatory elements of the *NFATc1* genomic locus (Misfeldt et al., 2009). NFATc1 is the only endocardial specific protein characterized in the embryo to date. Through manipulation of the Wnt/b-Catenin and BMP signaling pathways, Misfeldt *et al.* was able to enhance the differentiation of cardiomyocytes and promote the differentiation of endocardial cells from mESCs *in vitro* (Misfeldt et al., 2009, Palpant et al., 2015). Misfeldt *et al.* also identified a late Flk1+ mesodermal progenitor population that could give rise to endocardial, myocardial, endothelial, and smooth muscle lineages using clonal analysis (Misfeldt et al., 2009). Altogether, results from both *in vitro* and *in vivo* studies using various species provide credence to the existence of a multipotent progenitor population that can give rise to both endocardial cells and myocardial cells.

Endocardial, Vascular and Hematopoietic Endothelial Progenitors

Another model regarding the origin of endocardial cells states the myocardium and endocardium represent spatially separate populations within the cardiac mesoderm that develop in parallel (Fig 1.1). One study in support of the second theory was performed using the avian model. A retroviral construct consisting of the β-gal gene was introduced into mesodermal cells and injected into the precardiac region of embryos between HH stages 4 and 6 (Cohen-Gould et al., 1996). The injections only labeled ventricular cardiomyocytes. These results propose the bilateral precardiac mesoderm consists of cells that

are predestined to either an endocardial or myocardial fate, but not both. However, it is feasible that the two lineages diverged prior to labeling or that their fate was induced by positional cues (Eisenberg et al., 1995b).

Results from a zebrafish study also suggest endocardial cells derived from a distinct population of progenitors that also give rise to vascular and hematopoietic lineages. In this particular study, a mutation in the *cloche* gene prevented the formation of the endocardium and reduced the population of presumptive hematopoietic cells. Interestingly, the differentiation of cardiomyocytes as well as their contributions to a beating heart tube appeared unperturbed in the zebrafish mutant, though the primitive heart exhibited reduced contractility (Stainier et al., 1995, Harris et al., 2010). In another zebrafish study, single cell injections and tracking demonstrated myocardial progenitors were distributed throughout the margin of the early and midblastula embryo, while endocardial precursor cells were constrained to the most ventral marginal region of the heart field that also included progenitors of the hematopoietic and vascular endothelial lineages (Lee et al., 1994). Tracking of primitive endocardial cells in *vegfr4:gfp* zebrafish demonstrated that endocardial precursors derive from a region in the lateral plate mesoderm that also contributes to hematopoietic cells of the primitive myeloid lineage (Bussmann et al., 2007). Further investigation revealed that the primitive endocardial cells migrated from this region to the future location of the heart tube where they merged with the bilateral myocardial fields. In zebrafish *Scl/Tal1* mutant embryos the migration of pre-endocardial cells was hampered. Instead, the cells persisted as aggregates at the ventricular pole of the heart, whilst the migration of myocardial precursors remained uninhibited (Bussmann et al., 2007). In a 2011 avian study, DiI mapping was utilized to delineate endocardial progenitors in the chick embryo positioned in an area medial to the cardiac crescent and continuous with the endothelial plexus at HH stage 7 (Milgrom-Hoffman et al., 2011). The QH1 antibody was used to identify endocardial cells within the analogous area of a quail embryo that migrated from the arterial pole, an area peripheral to the heart field (Milgrom-Hoffman et al., 2011). When transplanted to the cardiac primordium of stage 8 chick host embryos, these cells were found to contribute solely to the endocardium and not the myocardium. Collectively, these studies provide evidence of endocardial progenitors that arise

from a mesodermal population with a fate-restricted early during cardiogenesis and distinct from myocardial progenitors.

D. Critical Endocardial-Myocardial Interactions During Heart Development

While the origin of endocardial cells is still up for discussion, it is well accepted that with time endocardial cells amalgamate to establish the inner layer of the primitive heart tube, which is separated from the outer layer of myocardium by an extracellular matrix known as the cardiac jelly. From that point on, the juxtaposition of the endocardium and myocardium persists throughout heart development and permits the cell-cell interactions that are essential for several key morphogenetic events.

Valvulogenesis and Septum Formation

During valve formation, endocardial cells within the atrioventricular canal (AVC) and proximal outflow tract (OFT) delaminate and invade the enlarged bilateral regions that separate the myocardium and endocardium. Valvulogenesis commences in response to adjacent signals from tissues such as the myocardium that prompt endocardial cells to undergo epithelial-mesenchymal transformation (EMT), migrate and proliferate (DeLaughter et al., 2011, Pucéat et al., 2013). Data from the Zhou laboratory suggest endocardial cells are involved in a reciprocal signaling network with the myocardium to stimulate mesenchymal transformation (Wang et al., 2013). Endocardial-specific Jagged1-Notch1 signaling promoted the expression of *Wnt4*, which in turn increased the expression of *Bmp2* in the adjacent AVC myocardium and consequently induced a subset of endocardial cells to undergo EMT (Wang et al., 2013). Early studies investigating the roles of NFATc1 revealed that null mutations resulted in the absence of aortic and pulmonary valves, in addition to ventricular septal defects (de la Pompa et al., 1998, Ranger et al., 1998, Chang et al., 2004). A more recent study demonstrated that the continuous expression of *NFATc1* is required in a subpopulation of endocardial cells to suppress Snail1 and Snail2 and thus prevent EMT (Wu et al., 2011). These cells are maintained as a proliferative group of the valve endocardium and will eventually contribute to elongation of the valve leaflet. Snail1 and Snail2 are also regulated by Erg,

an Ets factor greatly expressed in endothelial cells (Vijayaraj et al., 2012). Erg also inhibits VE-cadherin and is thus necessary for valvular endocardial cells to undergo EMT and migrate into the cardiac cushions (Vijayaraj et al., 2012). The primitive valves remodel into stratified leaflets through a multifaceted series of morphogenetic processes, signaling cascades, and mechanical events (Chakraborty et al., 2010). Heparin-binding EGF-like growth factor (HB-EGF) is a growth factor specifically expressed in untransformed endocardial cells that plays an important role later during valvulogenesis (Iwamoto et al., 2006). *HB-EGF* null mutations resulted in enlarged semilunar and AV valves of the heart, which suggests a role for this paracrine growth factor in the proliferation of mesenchymal cells and maintenance of endocardial cells during valve remodeling (Iwamoto et al., 2003).

Following transformation, endocardial cells also migrate into interventricular and atrial septal tissue (Chang et al., 2004). One study using the mouse model suggests endocardial cells play a role in the formation of the atrial septum. An increase in apoptosis among endocardial cells that lacked Tbx5 resulted in atrial septal defects (Nadeau et al., 2010). Further investigation by Nadeau *et al.* revealed an interaction between Tbx5, Gata4, and endocardial nitric oxide synthase (NOS) that promoted the survival of endocardial cells and the development of the atrial septum. Overall, valvulogenesis requires interactions between endocardial and myocardial cells to initiate a series of morphogenetic changes that are accompanied by the activation of multiple signaling cascades to ensure the proliferation, elongation, and stratification of primitive valves.

Trabeculation

The endocardium also interacts with the myocardium during ventricular myocardial trabeculation, whereby proliferation and differentiation of cardiomyocytes result in the expansion and extension of the myocardial wall into a network of finger-like protrusions into the ventricular lumen (Odiete et al., 2012). Subsequent to proteolytic cleavage from ventricular endocardial cells, Neuregulin-1 (Nrg1) binds to the ErbB4 receptor on the surface of the underlying myocardium and activates ErbB2 through dimerization (Pentassuglia et al., 2009). Mutations of Nrg1, ErbB2, or ErbB4 in the mouse model result in cardiac

defects and embryonic death at E10.5 (Gassmann et al., 1995, Lee et al., 1995, Meyer et al., 1995). In the absence of ventricular trabeculation, the murine heart develops abnormal AV valves and a large common ventricle. In the zebrafish model, endocardial Nrg1 signal through the ErbB2 receptor to initiate ventricular trabeculation (Zhang W et al., 2013). Endocardial-specific Notch signaling is also essential during ventricular trabeculation. The expression of Notch1 intracellular domain (N1ICD) expression can be detected in the endocardial lining of trabeculae as early as E9.5 and acts as a mediator upstream of signaling pathways that are important for trabeculation, including Nrg1 (Grego-Bessa et al., 2007, High et al., 2008). In endocardial cells, Hand2 acts upstream of Nrg1 in the Notch signaling pathway and is also essential in regulating trabeculation. Endocardial-specific deletion of *Hand2* in mice resulted in hypotrabeculated ventricles and intraventricular septum defects that were analogous to tricuspid atresia (VanDusen et al., 2014). Conversely, mice systemically lacking Fkbp1a, a ubiquitously expressed isomerase, displayed ventricular hypertrabeculation and noncompaction (Chen et al., 2013). Endocardial-specific ablation of *Fkbp1a* increased N1ICD activity in mice. Thus, Fkbp1a may play a role in negatively modulating Notch1 activity in endocardial cells (Chen et al., 2013). Collectively, results from various studies confirm the importance of endocardial-mediated signaling during trabeculation, primarily to promote myocardial morphogenesis and extension into the lumen.

Contributions of the Endocardium to the Coronary Vasculature

Coronary vessels are comprised of endothelial cells and smooth muscle cells that form a network of tube-like structures throughout the myocardium and are crucial in distributing oxygen to the ventricular compact zones and septa (Ishii et al., 2009). The source of endothelial cells that contribute to the coronary vasculature has become quite controversial (Tian et al., 2015). Results from a recent study utilizing *NFATc1*-mediated Cre lineage tracing revealed that endocardial cells contributed primarily to endothelial cells of the coronary arteries early in development (Wu et al., 2012). A subpopulation of ventricular endocardial cells located on the luminal surface in mice lacking either myocardial *VegfA* or endocardial *VegfR2* failed to generate the endothelium of intramyocardial coronary arteries or to undergo

coronary angiogenesis. Van Dusen *et al.* revealed a role for Hand2 in regulating, at least in part, endocardial contributions to the coronary vasculature. Endocardial-specific deletion of *Hand2* resulted in the increased density of coronary lumens due to the dysregulation of *VegfA*, *VegfR2*, *VegfR3*, and *Nrp1* (key components of Vegf signaling) (VanDusen et al., 2014). One study has recently reported on the contributions of the endocardium to most of the newly formed coronary vessels located in the inner myocardial wall of the heart postnatally (Tian et al., 2014). As a response to compaction of the trabeculae, endocardial cells undergo lineage conversion into a distinct subset of VECs within the coronary vasculature. Overall, the endocardium plays a critical role during two temporally distinct stages of coronary vessel development, the earliest of which involves interactions with the myocardium through the VEGF signaling pathway.

E. Overview

Given that the endocardium is continuously engaged with the myocardium via paracrine signaling during heart development, it is possible that interactions between endocardial and myocardial cells are not limited to the second half of gestation. Endocardial and myocardial cells are maintained in close proximity throughout *in vivo* and *in vitro* differentiation long after cardiac mesoderm differentiation. The juxtaposition of endocardial and myocardial cells may be necessary to permit continuous cell-cell interactions such as paracrine signaling from the endocardium to the myocardium to promote myocardial differentiation and maturation (Motoike et al., 2003, Masino et al., 2004, Kattman et al., 2006, Bu et al., 2009, Misfeldt et al., 2009, Pasquier et al., 2017).

Until recently, there has not been a developmental tool available that would permit the study of heart development in the absence of endocardial cells without affecting vascular endothelial cells due to the genetic profile shared between the two cell types. In an effort to circumvent this issue of specificity and to elucidate an earlier cell-cell interaction between endocardial and myocardial cells, we have generated a unique *in vitro* model that permits the ablation of endocardial cells. By taking advantage of the endocardial marker NFATc1 and the Diphtheria toxin receptor, we can study the consequence of

exclusively ablating endocardial cells on myocardial differentiation during the early stage of cardiogenesis. Chapter II describes the generation of an *NFATc1-DTR* BAC transgenic mouse embryonic stem cell line and the multiple experiments performed to validate *NFATc1-DTR* faithfully recapitulate endogenous *NFATc1* expression. Chapter II also consists of data that suggest the differentiation and maturation of cardiomyocytes *in vitro* is dependent on early communication with endocardial cells that involve the Bmp signaling pathway. Lastly, Chapter II ends with *in vivo* data from two *NFATc1* BAC transgenic mouse lines that demonstrate the specific expression of corresponding reporters within endocardial cells and their progeny. Chapter III concludes with a discussion regarding the significance of the findings from this study and future directions that will further our understanding about the novel interaction between endocardial and myocardial cells we discovered and how Bmp signaling is involved.

CHAPTER II

THE ABLATION OF ENDOCARDIAL CELLS THROUGH EXPRESSION OF THE *NFATc1-DTR* TRANSGENE IDENTIFIES AN EARLY ENDOCARDIAL-MYOCARDIAL INTERACTION THAT INVOLVES BMP SIGNALING

A. Introduction

Cell-cell interactions that occur during heart development *in vivo* can involve various factors and signaling pathways that have proven challenging to identify and investigate. The mESC *in vitro* model has been shown to mirror events that occur prior to and after gastrulation with high fidelity. Thus, mESCs are acceptable for studying the various molecular, cellular, and developmental processes of early embryogenesis (Misfeldt et al., 2009, Schulz et al., 2009, Van Vliet et al., 2012, DeLaughter et al., 2016). Most importantly, the use of mESCs has proven to be an efficient alternative method by which we can study interactions that occur between myocardial and endocardial cells. By utilizing bacterial artificial chromosome (BAC) recombineering, we were able to generate a mESC transgenic line that expresses a nuclear enhanced green fluorescent protein (GFP) reporter and the human HB-EGF [also known as the Diphtheria toxin receptor (DTR)] under the transcriptional regulatory elements of the *NFATc1* genomic locus. Following the differentiation of this BAC transgenic line (*NFATc1-DTR*), we were able to detect expression of the GFP reporter, which recapitulated the expression of endogenous NFATc1 in endocardial cells. However, as a result of cell death induced in endocardial cells within *NFATc1-DTR* EBs treated with Diphtheria toxin (DT) during differentiation, expression of the reporter and endogenous NFATc1 was not detected. Therefore, the *NFATc1-DTR* mESC line is an efficient developmental tool for identifying and studying endocardial-myocardial interactions as well as for elucidating the roles of these interactions in the differentiation and maturation of cardiomyocytes.

B. Experimental Procedures

Generating the NFATc1-DTR ESC Line

The *NFATc1-DTR* BAC transgene was generated utilizing a multicistronic vector that includes a nuclear localized GFP reporter (H2B-eGFP) and the human Heparin Binding EGF Like Growth Factor (HBEGF) (also known as the diphtheria toxin receptor) fused by a self-cleaving 2A peptide (Mitamura et al., 1995, Donnelly et al., 2001, Stewart et al., 2009). The *NFATc1-DTR* transgene was introduced into homologous arms of the mouse *NFATc1* gene between the 500 bp 5' translational start site and the 400 bp 3' splice site of exon 1. BAC recombineering of the *NFATc1-DTR* transgene into the whole NFATc1 genomic locus was accomplished using a previously described protocol (Lee et al., 2001). Following recombination, the transgene was first purified through a cesium chloride gradient and then dialyzed with the use of microinjection buffer (10 mM Tris, 15 μM EDTA pH 7.4). The *NFATc1-DTR* transgene was then electroporated into G4 F_1 hybrid ESCs that were generously provided by Dr. Andras Nagy (Lunenfeld-Tanenbaum Research Institute, ON, Canada) (George et al., 2007). ESCs that efficiently incorporated the *NFATc1-DTR* BAC transgene and the neomycin-resistance cassette were cultured on irradiated mouse embryonic fibroblasts (MEFs), that also consisted of the neomycin-resistance cassette (Millipore PMEF-NL), and treated with 500ug/ml of G418 Sulfate (Corning) prior to the selection of potential clones.

Generating the BAC Transgenic Mouse Lines

Eight *NFATc1-DTR* BAC ESCs were inserted into the space between the zona pellucida and blastomeres of 2.5 dpc, 8-cell ICR mouse (*Mus musculus, Mm*) embryos utilizing the laser-assisted microinjection method (Poueymirou et al., 2007). After a twenty-four hour incubation at 37^{o}C, the 3.5 dpc (days post coitum) embryos were transferred into the uterine horns of pseudo-pregnant ICR dams where they continued to develop until birth. The *NFATc1-Cre* BAC transgenic mouse line was generated utilizing the PiggyBac transgenic method by Cyagen Biosciences Inc. (Guangzhou, China). F0 chimeric males that exhibited 100% coat color and genotyped positive for the transgene were then mated with

C57BL/6 dams to propagate F1 generation litters. All the mice were maintained in agreement with protocols approved by the Vanderbilt University Animal Care and Use Committee (IACUC).

Expansion and Differentiation of NFATc1-DTR ESCs

NFATc1-DTR ESCs were cultured on neomycin-resistant MEFs with media that contained Dulbecco's Modified Eagle Medium (DMEM-Invitrogen) accompanied with 4.5g/L of D-Glucose and 2mM of L-glutamine. The media also consisted of 15% FBS (Atlanta Biologicals), 100 μM non-essential amino acids, 1 mM sodium pyruvate, 100 μM β-mercaptoethanol, 100 U/ml Pen/Strep, and 1000 U/ml recombinant leukemia inhibitory factor (ESGRO mLIF, Millipore). Hanging drops of $2.5x10^{-4}$ *NFATc1-DTR* ESCs cultured in differentiation media (DM) were incubated in 37°C for forty-eight hours in order to form embryoid bodies (EBs). The DM consisted of Iscove's Modified Dulbecco's Medium (IMDM) complemented with 2mM L-glutamine and 25 mM HEPES. The differentiation media also contained 15% FBS (Atlanta Biologicals), 0.5 mM L-ascorbic acid (Sigma), 100 U/ml Pen/Strep, 15 μg/ml transferrin (Roche), and $4.5x10^{-4}$ M 1-thioglycerol. The EBs were cultured in suspension with media utilizing non-treated suspension culture dishes from day 2 to day 4 of differentiation prior to being transferred onto 0.1 % gelatinized culture dishes on day 4 of differentiation. The EBs were maintained on the gelatinized dishes for the remainder of the differentiation while the media was changed every forty-eight hours. The EBs were treated with Diphtheria toxin (Sigma, 0.1 μg/ml), rhBmp2 (R&D, 100 ng/ml), rhBmp4 (10 ng/ml), Tgfβ1 (5 ng/ml), Igf1 (100 ng/ml), Nrg1b1 (100 ng/ml), Pdgfb (10 ng/ml), Noggin (150 ng/ml), Grem 2 (100 ng/ml), or Fgf3 (10 ng/ml).

RNA Analysis Through Reverse Transcription, cDNA Synthesis, and Quantitative RT-PCR (qPCR)

Total RNA was isolated from *NFATc1-DTR* EBs in accordance with the TRIzol protocol (Invitrogen). One milligram of RNA treated with DNase I (Invitrogen) before reverse-transcribed into cDNA in accordance with the SuperScript III first-strand synthesis system protocol (Invitrogen). The cDNA was then analyzed using qPCR with SsoAdvanced Universal SYBR Green Supermix (BioRad) and

gene-specific primers. The cycling conditions were as follows: 94^{o} for 5 min, 94^{o} for 1 min, and 35 cycles of amplification (94^{o} denaturation for 30 s, 55^{o} annealing for 30s, 72^{o} elongation for 60 s) using the C1000 Touch Thermal Cycler (BioRad). The qPCR experiments were performed in triplicates. Relative expression was calculated as $2^{-\Delta\Delta CT}$ with the use of 18s as an internal control.

Immunofluorescence and Fluorescent Microscopy of Embryoid Bodies and Sectioned Embryos

For immunofluorescence experiments, EBs cultured in 8-well chamber slides (Nunc, Lab-Tek) from day 4 of differentiation were fixed with 2% paraformaldehyde (PFA) and blocked in 0.1 % PBST with 5% BSA (Sigma) and 10% normal goat serum (NGS). The EBs were then incubated with primary antibodies overnight at 4^{o}C. Cryosections (10 μm) of *NFATc1-DTR* and *NFATc1-mCherry* embryos were fixed in 4% PFA before they were incubated in blocking solution consisting of 2% paraformaldehyde (PFA) and blocked in 0.1 % PBST with 5% BSA (Sigma) and 10% normal goat serum (NGS). The sections were then incubated with primary antibodies overnight at 4^{o}C. Primary antibodies included; GFP (Invitrogen 1:200, rabbit # A-11122), MHC (DSHB 1μg/ml, mouse MF20), cTnT (Developmental Studies Hybridoma Bank [DSHB] 1μg/ml, mouse CT3), CD31/Pecam-1 (BD Pharmingen 1:150, rat MEC13.3 # 550274) and pHH3 (CST 1:200, rabbit # 9701). Sections that were stained with the NFATc1 antibody (BD Pharmingen 1:50, mouse 7A6 # 556602) were processed in accordance with the mouse on mouse (M.O.M.^{TM}) immunodetection kit protocol (Vector Labs). Cell death was detected in *NFATc1-DTR* EBs with the use of The ApopTag® Red In Situ Apoptosis Detection kit and in accordance with the TUNEL protocol (Millipore). All the samples were incubated in Alexa Fluor^{TM} conjugated secondary antibodies for 1 hour in the dark at room temperature and then mounted with the ProLong Gold Antifade Mountant with DAPI (Life Technologies). An image of the stained samples was captured using an Olympus FV-1000 inverted confocal microscope or a Nikon Eclipse E800 epifluorescence microscope. Adobe Photoshop CS6 was used to analyze images of the stained samples and for quantitative purposes. The average of the total number of proliferating and dying cells between 3 frames per sample within the control and treated groups of three biological replicates was determined and graphed.

β-galactosidase (LacZ) Staining of Whole-Mount Embryos

E10.0 *NFATc1-Cre; Rosa26*^{LacZ} embryos were initially dissected in cold phosphate-buffered saline (PBS) and fixed in 4% PFA for 4 hours at 4^{o}C. The embryos were then incubated overnight at 37^{o}C in X-gal staining buffer that consisted of 1 mg/ml X-gal, 0.02% NP40, 5 mM potassium Ferro/Ferricyanate, 2 mM Magnesium Chloride, and 0.01% sodium deoxycholate in PBS. Embryos were then washed and dehydrated using a series of ethanol and Xylene before processed for embedding in paraffin. Sections of the embryos (6 μm) were incubated in Xylene, rehydrated in ethanol, and stained with Eosin Y before imaged with a Nikon AZ 100 M microscope.

Flow Cytometry and Fluorescence-Activated Cell Sorting (FACS) of NFATc1-mCherry EBs

NFATc1-mCherry ESCs were differentiated using the same hanging drop protocol previously mentioned. On the eighth day of differentiation, *NFATc1-mCherry* EBs were dissociated using cell dissociation buffer (Gibco) and resuspended in a solution containing Hanks' Buffered Salt Solution (HBSS), 25mM HEPES, and 2% FBS. To prevent nonspecific binding, the cells were first incubated with CD16/CD32 (mouse, Ebiosciences, 1 μg/ml) and then incubated with an Allophycocyanin-conjugated (APC) antibody against CD31/Pecam-1 (Rat Anti-Mouse MEC 13.3, BD Pharmingen, 0.5 μg/ml). In an attempt to isolate and eliminate dead cells from the collection, the cells were also stained with propidium iodide (PI) (Molecular Probes). Endocardial cells (mCherry^{+}/CD31^{+}) and endothelial cells (mCherry^{-}/CD31^{+}) were physically sorted out from the heterogeneous *NFATc1-mCherry* population of 3x10^{6} cells per 1ml with the use of the FACSAria^{TM} from Becton Dickinson and the FACSDiva^{TM} 6.0. RNA was isolated from sorted cells using a Qiagen RNeasy Mini Kit (Cat No: 74104, Lot No: 145038477) in accordance with the manufacturer's instructions. RNA quality was obtained using a Tapestation high sensitivity assay where a RIN value of at least 8.0 was required and submitted for RNAseq analysis.

Statistical Analyses

Statistical data presented in the current study represent the mean ± standard error of the mean (SEM). A two-tailed Student's *t*-test was used to identify statistical significance in the difference of mean values compared during quantitative analyses. Differences were considered significant if $P < 0.05$. The sample size represents a collection of biological replicates.

C. Results

Endocardial Cells are Efficiently Depleted Following DT Treatment of NFATc1-DTR EBs During Differentiation in vitro

Crosstalk between endocardial and myocardial cells is known to occur during the later stages of heart development, but it is unknown whether such an interaction occurs during the very early stages shortly after gastrulation. We have attempted to address this dearth in information relating to heart development by generating an experimental *in vitro* model that will allow us to identify additional endocardial-myocardial interactions. With the use of BAC recombineering, we were able to introduce both the Diphtheria toxin receptor (DTR) and an enhanced green fluorescent protein reporter (GFP) into the genomic locus of *NFATc1* (Fig. 2.1A) to generate a transgene that will permit DT-induced cell death of endocardial cells when expressed. Following electroporation of the *NFATc1-DTR* BAC transgene into low passage G4 hybrid mESCs, the surviving cells underwent G418 selection and expansion (Tompers et al., 2004, George et al., 2007). Once established as a viable line, *NFATc1-DTR* mESCs were then differentiated using the hanging drop method (Fig. 2.1B).

Expression of the GFP reporter could be detected as early as day 6 (D6) of differentiation in *NFATc1-DTR* EBs. Immunofluorescent (IF) staining revealed GFP expression colocalized with $NFATc1^+$ cells (Fig. 2.1C, D). The additional staining for endothelial cells using CD31/Pecam-1^+ (CD31) confirmed that the $GFP^+/NFATc1^+$ endocardial cells represented a distinct population of the endothelium (Fig. 2.1E) (Misfeldt et al., 2009). Expression of the GFP reporter could also be detected later in differentiation

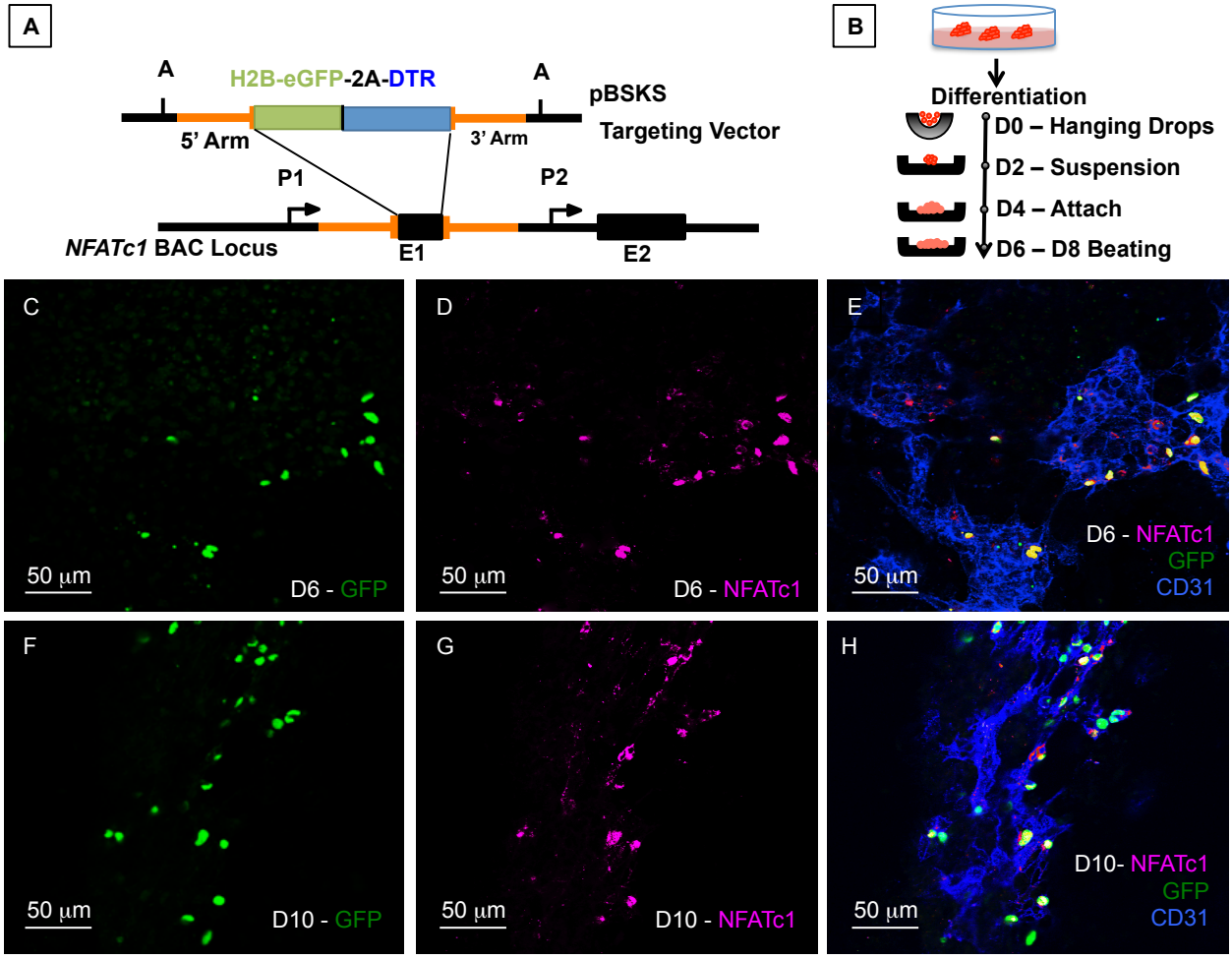

Figure 2.1. Expression of *NFATc1-DTR* faithfully recapitulates endogenous *NFATc1* expression within endocardial cells.

(A) A transgene consisting of a nuclear GFP reporter and DTR (H2B-GFP-2A-DTR) was introduced into the genomic locus of *NFATc1* using BAC recombineering. AscI site, A; pBluescript KS+, pBSKS; P1 promoter, P1; P2 promoter, P2; Exon1, E1; Exon2, E2. (B) GFP expression was detected in D6 *NFATc1-DTR* EBs within endocardial cells that also expressed (C) endogenous NFATc1 and (D) CD31. The expression of (E) GFP, (F) NFATc1, and (G) CD31 also labeled endocardial cells in D10 *NFATc1-DTR* EBs.

within D10 EBs using immunofluorescence. The nuclear expression of GFP coincided with the endogenous expression of both NFATc1 and CD31 (Fig. 2.1F-H). From these results, we can conclude that expression of the *NFATc1-DTR* transgene faithfully recapitulate endogenous NFATc1 expression and is constrained to the endocardium that is clearly distinct from the remaining vascular endothelium.

Following verification of the endocardial-restricted expression of the *NFATc1-DTR* transgene, we proceeded to test the specific expression and function of the diphtheria toxin receptor. Endocardial cells within *NFATc1-DTR* EBs were ablated from D0 to D6 of differentiation by introducing DT into the culture media. The expression of GFP was clearly detected in non-treated $NFATc1^{+}/CD31^{+}$ endocardial cells and absent in *NFATc1-DTR* EBs treated with DT from D0 to D6 (Fig. 2.2A, B). The number of $NFATc1^{+}$ cells that was also attenuated within DT-treated *NFATc1-DTR* EBs confirms the successful ablation of endocardial cells. Quantification of immunofluorescent staining demonstrated that DT-induced ablation specifically reduced the number of $NFATc1^{+}$ endocardial cells present within D6 *NFATc1-DTR* EBs without overtly disrupting the number of $CD31^{+}$ endothelial cells within DT-treated EBs relative to the control (Fig. 2.2C). To ensure the ability to ablate endocardial cells was not limited to a specific time frame *in vitro*, we next treated *NFATc1-DTR* EBs with DT from D0 to D10 of differentiation. The extended ablation greatly diminished the number of $CD31^{+}/NFATc1^{+}/GFP^{+}$ endocardial cells present when compared to those detected in untreated EBs (Fig. 2.2D, E) as demonstrated by IF. Quantification of cells that expressed the GFP reporter and endogenous NFATc1 supported the observation regarding a decrease in endocardial cells as a result of DT treatment and confirmed the overall vascular endothelium ($CD31^{+}$) remained unperturbed in D10 EBs (Fig. 2.2F). Overall, these results confirm that expression of the GFP reporter is endocardial-specific and recapitulates endogenous *NFATc1* expression. We can also conclude that DT treatment of *NFATc1-DTR* EBs efficiently ablated in endocardial. Additionally, the remaining endothelial populations, as well as lineages derived from the endodermal and ectodermal germ layer, were not affected by DT treatment (Fig 2.3 A-D).

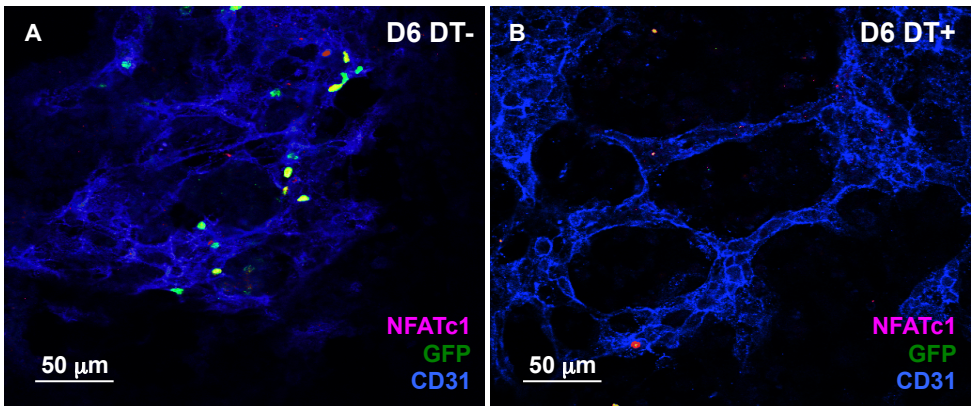
A
D6 DT-
NFATc1
GFP
CD31
50 µm
B
D6 DT+
NFATc1
GFP
CD31
50 µm

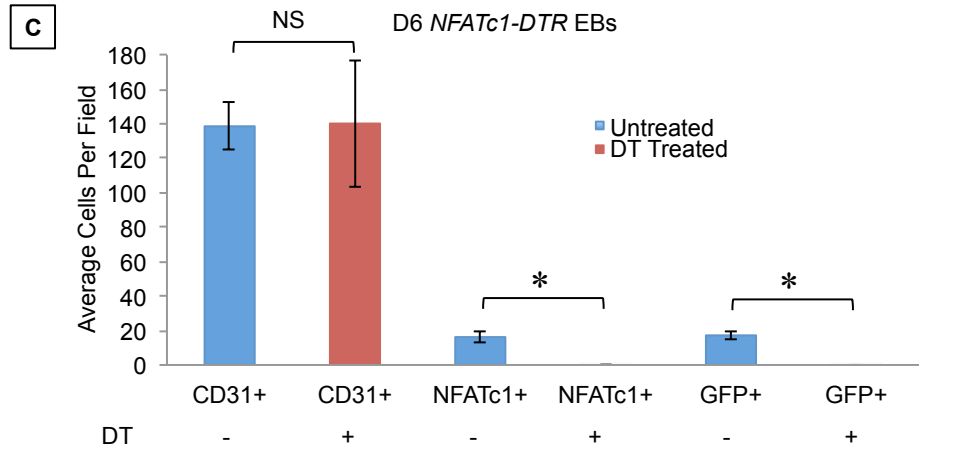
C
D6 NFATc1-DTR EBs
NS
Average Cells Per Field
180
160
140
120
100
80
60
40
20
0
Untreated
DT Treated
*
*
CD31+
CD31+
NFATc1+
NFATc1+
GFP+
GFP+
DT
-
+
-
+
-
+

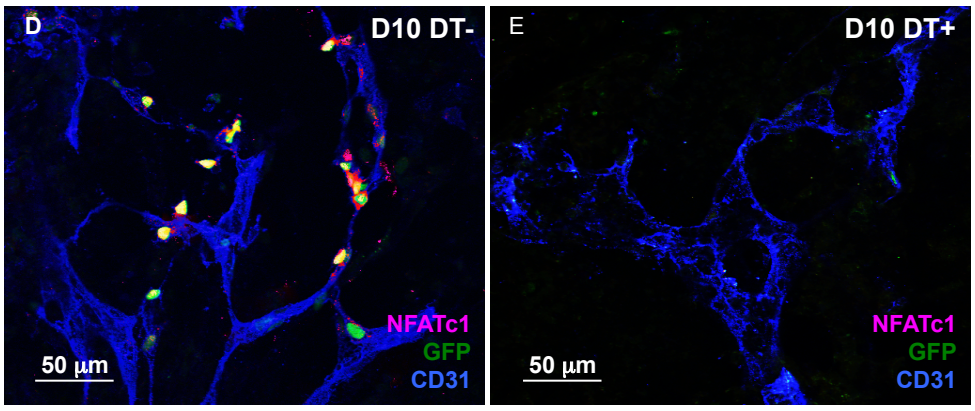
D
D10 DT-
NFATc1
GFP
CD31
50 µm
E
D10 DT+
NFATc1
GFP
CD31
50 µm

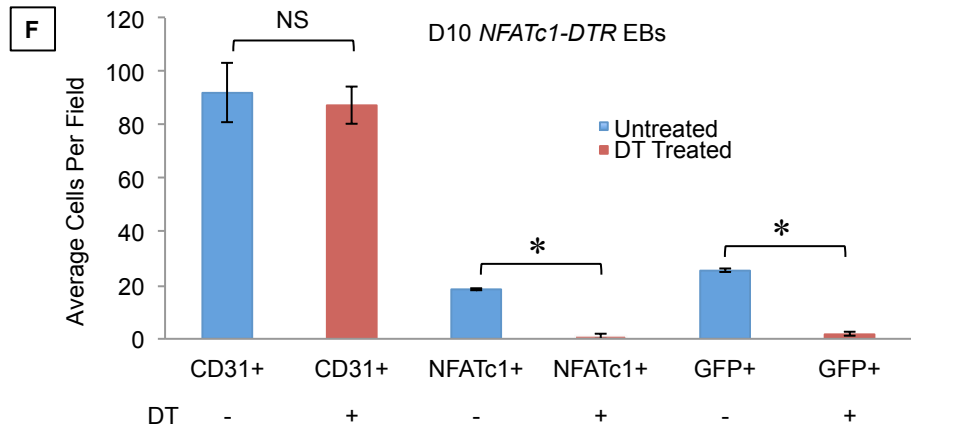
F
D10 NFATc1-DTR EBs
NS
Average Cells Per Field
120
100
80
60
40
20
0
Untreated
DT Treated
*
*
CD31+
CD31+
NFATc1+
NFATc1+
GFP+
GFP+
DT
-
+
-
+
-
+

Fig 2.2. Diphtheria toxin treatment specifically ablates NFATc1$^+$/GFP$^+$/CD31$^+$ endocardial cells.

(A) Endocardial cells labeled according to their expression of GFP, NFATc1, and CD31 in untreated D6 *NFATc1-DTR* EBs were mostly absent in D6 EBs (B) treated with DT from D0 to D6 of differentiation. (C) Quantification of the IF results regarding NFATc1$^+$, GFP$^+$, and CD31$^+$ cells present per field in untreated and DT-treated D6 *NFATc1-DTR* EBs was graphed. (D) NFATc1$^+$/GFP$^+$/CD31$^+$ endocardial cells present in untreated D10 *NFATc1-DTR* EBs were also successfully ablated following DT treatment from D0 to D10 (E). (F) The decrease in NFATc1$^+$ and GFP$^+$ cells detected in DT-treated D10 EBs was also quantified and graphed. N=3. Error bars indicate SEM.

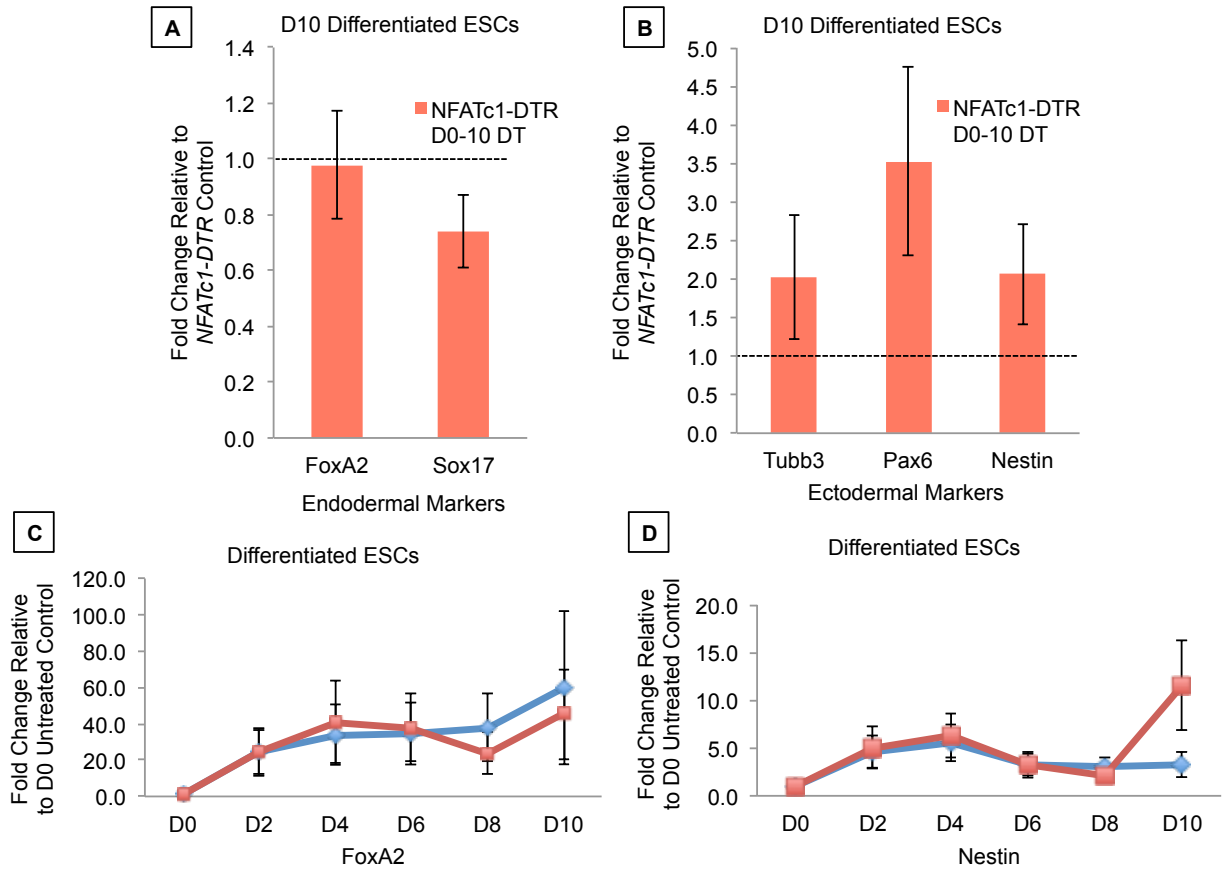

Fig 2.3. DT treatment has no overall effect on the differentiation of ectodermal and endodermal lineages.

(A) The expression of endodermal markers FoxA2 and Sox17 were not greatly affected by DT treatment in *NFATc1-DTR* EBs. (B) DT treatment appeared to have a favorable, albeit insubstantial influence on the expression of ectodermal markers Tubb3, Pax6, and Nestin in *NFATc1-DTR* EBs. (C, D) The temporal expression of both FoxA2 and Nestin appeared to be very similar between the untreated and DT-treated *NFATc1-DTR* EBs. There was, however, an unexpected peak detected in the expression of Nestin in D10 DT-treated *NFATc1-DTR* EBs. N=3. Error bars indicate SEM.

Endocardial Ablation Decreases Myocyte Differentiation, Maturation, and Function in vitro

To investigate the consequences of ablating endocardial cells on the differentiation of myocardial cells, we first considered a functional assessment of myocytes within untreated and DT-treated EBs. *NFATc1-DTR* ESCs and WT G4 ESCs were treated with DT from D0-D10 of differentiation. G4 ESCs served as a good WT control since they were used to make the transgenic line. Overall, DT treatment of WT EBs did not appear to overtly affect the percent of contracting foci compared to untreated WT EBs, though there was a slight decrease detected on D8 (Fig. 2.4A). Conversely, the number of beating myocytes detected within DT-treated *NFATc1-DTR* EBs was significantly reduced compared to untreated *NFATc1-DTR* EBs on D8 and D10 of differentiation (Fig. 2.4B). Thus, we can conclude that in spite of the similar behavior observed in contracting myocytes between untreated *NFATc1-DTR* EBs and untreated as well as DT-treated WT EBs, the presence of DTR permitted the specific DT-mediated ablation of $NFATc1^{+}$ endocardial cells. Additionally, the ablation of endocardial cells appeared to disrupt an essential endocardial-myocardial interaction and significantly reduced the number of contracting EBs (Mitamura et al., 1995).

To determine if the decrease in beating cardiomyocytes detected in DT treated D10 *NFATc1-DTR* EBs was due to a change in myocyte gene expression, we first analyzed the expression of early cardiomyocyte differentiation markers. The expression of *Nkx2.5, Isl1*, *Gata4*, *Gata6*, *Hand1*, and *Hand2* were all decreased in DT-treated *NFATc1-DTR* EBs (Fig. 2.4C) (Tanaka et al., 1999, Cai et al., 2003, Lescroart et al., 2014). Markers demarcating mature myocytes including *cTnT, αMHC, Mlc2a*, and *Mlc2v* were also greatly reduced in D10 DT-treated *NFATc1-DTR* EBs (Lyons et al., 1990, O'Brien et al., 1993, Kubalak et al., 1994) (Fig. 2.4D). These results suggest a role for the endocardium in maintaining a population of cardiomyocytes that continues to express the early myocardial markers of differentiation or to promote the maturation of these cells and thus may explain why DT-treatment of *NFATc1-DTR* EBs yielded fewer differentiating myocytes maturing into functional contractile myocardium.

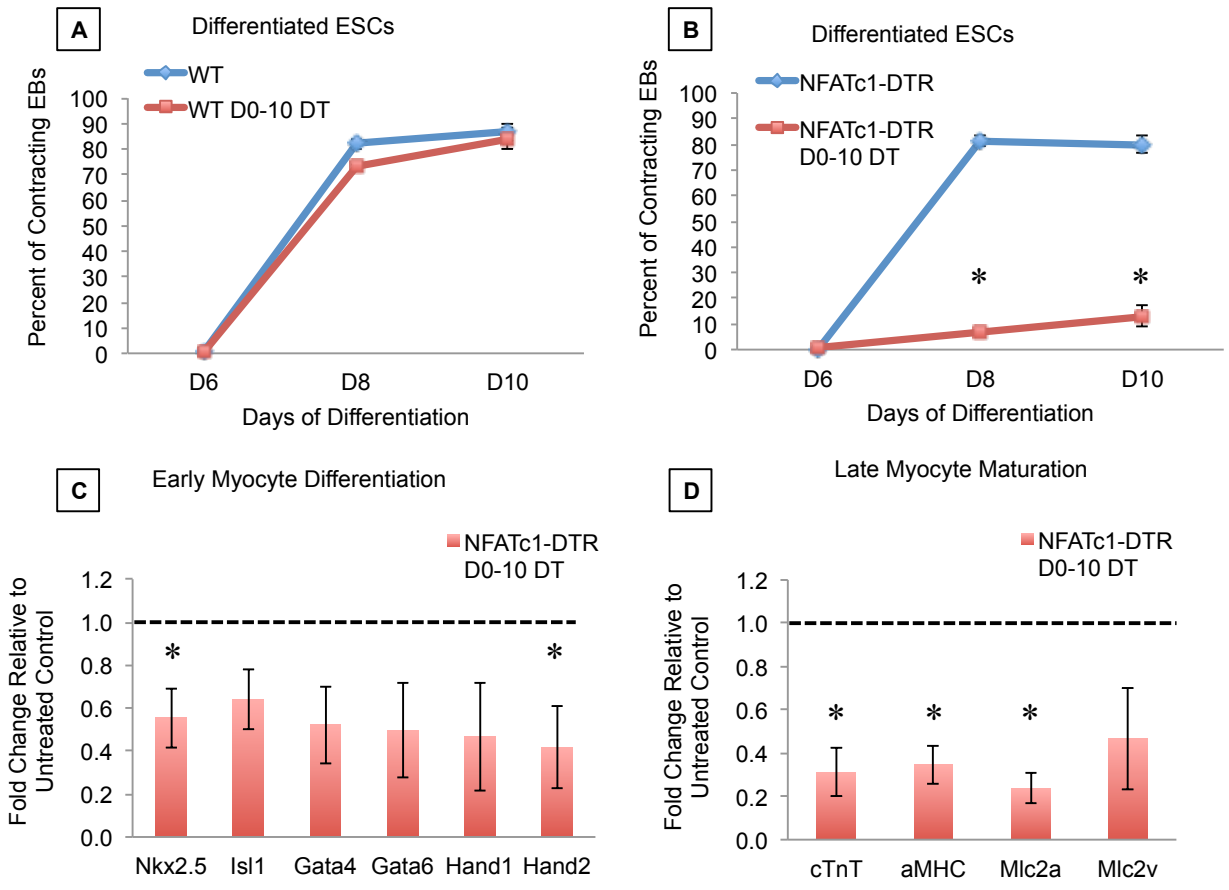

Fig 2.4. Endocardial ablation reduces the differentiation and function of cardiac myocytes in *NFATc1-DTR* EBs.

(A) DT treatment slightly reduced the percentage of contracting myocytes in WT EBs relative to untreated WT EBs. (B) The treatment of *NFATc1-DTR* EBs with DT significantly reduced the percent of beating cardiomyocytes detected on D8 and D10 compared to untreated *NFATc1-DTR* EBs. Concurrent with the decrease in contracting cardiomyocytes, qPCR analysis revealed the reduced expression of myocyte (C) differentiation and (D) maturation markers in D10 DT-treated *NFATc1-DTR* EBs. *=$p< 0.05$ vs. control, N=3. Error bars indicate SEM.

There is a Specific Developmental Window in Which Endocardial-Myocardial Interactions are Essential for the Differentiation and Maturation of Cardiomyocytes in vitro

To further delineate the underlying cause for the decrease in beating cardiomyocytes and expression of myocyte differentiation markers detected in DT-treated *NFATc1-DTR* EBs, we next considered if there were any changes in the proliferation or cell death of myocardial cells due to endocardial ablation. IF staining for the proliferation marker phosphor-HistoneH3 (pHH3) was used to identify proliferating cardiomyocytes stained with cardiac myosin heavy chain (MHC) in D6 untreated *NFATc1-DTR* EBs and *NFATc1-DTR* EBs treated with DT from D0 to D6 (Fig. 2.5A, B). Quantification of the IF analyses demonstrated that though there were fewer MHC^+ cardiomyocytes per field as a result of DT treatment in *NFATc1-DTR* EBs, the number of proliferating cardiomyocytes that expressed both $pHH3^+$ and MHC^+ did not differ between untreated and DT-treated *NFATc1-DTR* EBs (Fig. 2.5C).

Next, we used TUNEL staining to determine whether cell death among cardiomyocytes was affected by DT treatment in D6 *NFATc1-DTR* EBs. Results from the TUNEL fluorescence assay revealed that the decrease in MHC^+ cardiomyocytes present in *NFATc1-DTR* EBs treated from D0 to D6 relative to untreated *NFATc1-DTR* EBs could not be attributed to cell death (Fig. 2.5D, E). Quantification of the IF analysis confirmed there was a similar number of dying $MHC^+/TUNEL^+$ cardiomyocytes in both control and DT-treated D6 *NFATc1-DTR* EBs (Fig. 2.5F). From these results, we can deduce that the ablation of endocardial cells in *NFATc1-DTR* EBs reduced the number of cardiomyocytes present at D6 without affecting the overall proliferation or cell death of cardiomyocytes.

Given that endocardial ablation appeared to affect the expression of key myocyte differentiation markers, we next sought to identify the time frame in which myocardial cells are initially dependent on interactions with endocardial cells for differentiation. *NFATc1-DTR* EBs were treated with DT during various time intervals that ranged from two to ten days. Among the different time intervals tested, the decrease in contracting myocytes within *NFATc1-DTR* EBs treated with DT from D4 to D8 of

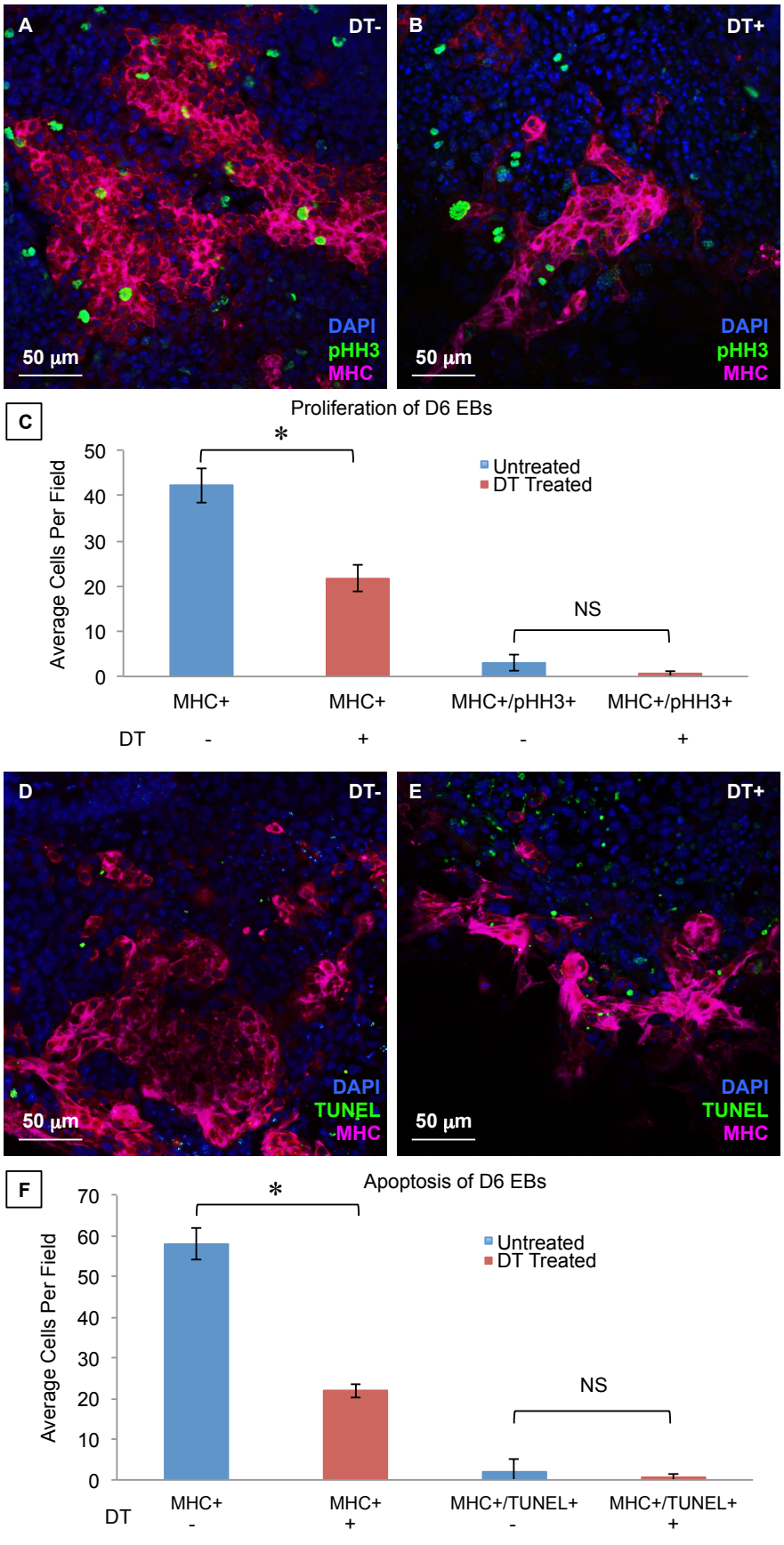
A
DT-
DAPI
pHH3
MHC
50 µm
B
DT+
DAPI
pHH3
MHC
50 µm
C
Proliferation of D6 EBs
Average Cells Per Field
50
40
30
20
10
0
*
Untreated
DT Treated
NS
MHC+
MHC+
MHC+/pHH3+
MHC+/pHH3+
DT
-
+
-
+
D
DT-
DAPI
TUNEL
MHC
50 µm
E
DT+
DAPI
TUNEL
MHC
50 µm
F
Apoptosis of D6 EBs
Average Cells Per Field
70
60
50
40
30
20
10
0
*
Untreated
DT Treated
NS
DT
MHC+
-
MHC+
+
MHC+/TUNEL+
-
MHC+/TUNEL+
+

Figure 2.5. Endocardial ablation decreases the number of cardiomyocytes present in D6 *NFATc1-DTR* EBs without decreasing proliferation or increasing cell death.

(A) IF analysis demonstrated that the number of MHC^+ cardiomyocytes in D6 *NFATc1-DTR* EBs was reduced in (B) *NFATc1-DTR* EBs treated with DT from D0 to D6 of differentiation. (C) Assessment of IF staining revealed there was no difference in the number of proliferating cardiomyocytes ($MHC^+/pHH3^+$) between untreated and DT-treated *NFATc1-DTR* EBs. There was no visible difference detected in the number of MHC^+ cardiomyocytes undergoing cell death between (D) untreated D6 *NFATc1-DTR* EBs and (E) *NFATc1-DTR* EBs treated with DT from D0 to D6. (F) Quantification of $MHC^+/TUNEL^+$ cells confirmed the decrease in MHC^+ cardiomyocytes present in DT-treated *NFATc1-DTR* EBs was not the result of an increase in cell death. *=$p< 0.05$ vs. control. Error bars indicate SEM. N=3.

differentiation was most similar to the decrease detected in *NFATc1-DTR* EBs treated with DT from D0 to D10 (Fig. 2.6A). The significant decrease in the percent of beating cardiomyocytes in *NFATc1-DTR* EBs treated with DT from D4-D8 of differentiation compared to untreated *NFATc1-DTR* EBs was detected as early D8 and continued to D10 (Fig. 2.6B). The decrease in beating myocardial cells observed in *NFATc1-DTR* EBs treated with DT from D4-D8 is congruent with the decreased expression of myocyte maturation markers in D10 EBs (Fig. 2.6C).

To further delineate the developmental window differentiating cardiomyocytes are most sensitive to the absence of endocardial cells we next analyzed and compared the temporal expression of key myocyte differentiation markers in untreated *NFATc1-DTR* EBs and *NFATc1-DTR* EBs treated with DT from D0 to D10. Given that we detected a decrease in the expression of multiple myocyte contractile markers in D10 *NFATc1-DTR* EBs treated with DT from D4 to D8, we first performed a temporal analysis of myocardial maturation marker *βMHC* (Boheler et al., 2002). Under untreated conditions, the temporal expression of *βMHC* appeared to increase by D8 of differentiation, which continued up to D10 in untreated *NFATc1-DTR* EBs (Fig. 2.7A). This increase in expression appeared to occur within the D4 to D8 time frame during which endocardial-myocardial interactions was observed to be critical for myocardial function. The treatment of *NFATc1-DTR* EBs with DT from D0-D10 significantly reduced the expression of *βMHC* relative to the control (Fig. 2.7A). The temporal expression of early myocyte differentiation markers *Nkx2.5* (Fig. 2.7B), *Mef2c* (Fig. 2.7C), and *Isl1* (Fig. 2.7D) in untreated *NFATc1-DTR* EBs also increased within the D4 to D8 time frame. This increase in temporal expression was significantly truncated as a result of DT treatment from D0 to D10. According to these results, we can conclude that the D4 to D8 time window, which encompasses the initial expression of both early and late markers of myocyte differentiation, involves interactions between endocardial and myocardial cells that when perturbed negatively affects the differentiation and maturation of cardiomyocytes.

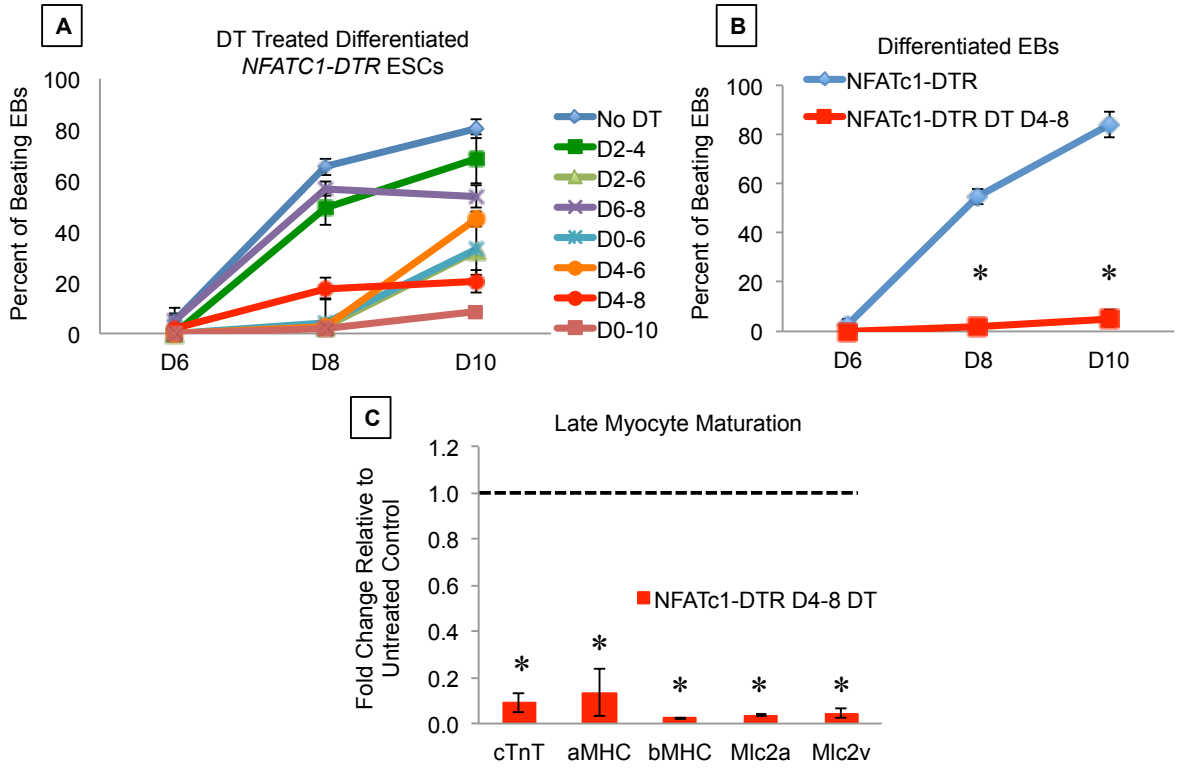

Figure 2.6. DT treatment of *NFATc1-DTR* EBs between D0 to D10 and D4 to D8 of differentiation results in a similar decrease in the number of contracting EBs and in the expression of myocyte contractile markers.

(A) *NFATc1-DTR* EBs were treated with DT during several, different time intervals of differentiation. A decrease in the percent of contracting myocytes was most similar between *NFATc1-DTR* EBs that were treated with DT from D4 to D8 and *NFATc1-DTR* EBs that were treated with DT from D0 to D10. (B) A significant decrease in contracting myocytes within *NFATc1-DTR* EBs treated with DT between D4 and D8 of differentiation was detected at D8 and D10. (C) The expression of key contractile markers was also decreased as a result of DT treatment of *NFATc1-DTR* EBs from D4 to D8. *=p< 0.05 vs. control. N=3. Error bars indicate SEM.

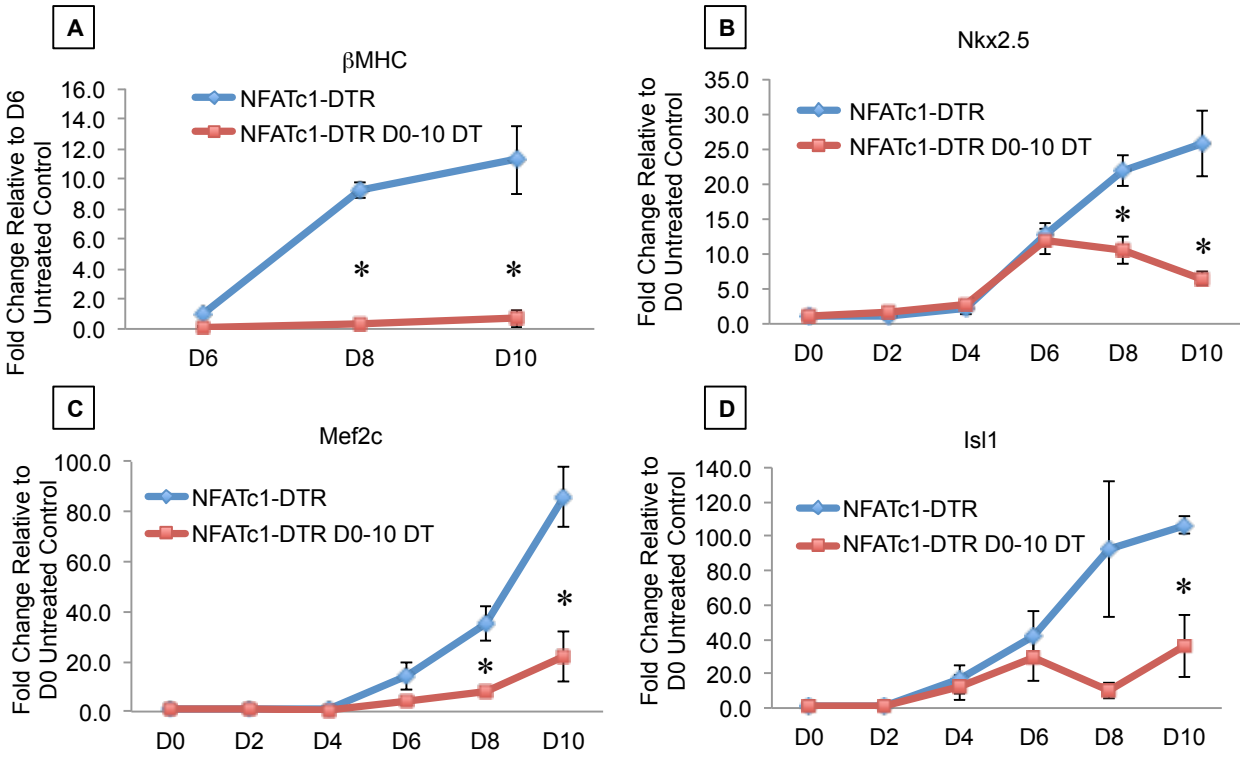

Figure 2.7. The D4 to D8 time frame in which myocardial differentiation relies on signaling from the endocardium coincides with the increased temporal expression of key myocyte markers.

(A) qPCR analysis regarding the temporal expression of βMHC revealed an initial increase on D8 that continued to D10. The increase in βMHC expression on D8 and D10 was significantly reduced due to DT treatment of *NFATc1-DTR* EBs. The temporal expression of (B) *Nkx2.5*, (C) *Mef2c*, *and* (D) *Isl1*, markers that represent early myocardial differentiation was initiated between D4 and D8 in untreated *NFATc1-DTR* EBs and greatly decreased in DT-treated *NFATc1-DTR* EBs. *=p< 0.05 vs. control. N=3. Error bars indicate SEM.

Bmp2 Treatment Partially Restores Myocardial Function and the Expression of Key Myocardial Markers During Endocardial Ablation

After identifying a time frame during *in vitro* differentiation in which cardiomyocytes are dependent on the presence of endocardial cells, we next sought to elucidate why this interaction is required. Given the various signaling pathways reported to be involved in endocardial-myocardial interactions, we first considered components of these signaling pathways as potential candidates. Furthermore, we wanted to focus on coinciding ligands highly expressed in endocardial cells. In order to obtain this information, we first needed access to a genetic profile that was specific to endocardial cells and separate from vascular endothelial cells. We decided to accomplish this task with the use of another BAC transgene at our disposal. *NFATc1-mCherry* ESCs consists of an *NFATc1* BAC transgene that, when expressed, results in the endocardial specific expression of a nuclear cyan reporter and a membrane-anchored mCherry (Fig. 2.8A) (Misfeldt et al., 2009). To confirm the *NFATc1-mCherry* transgene recapitulated published expression patterns of endogenous NFATc1 *in vivo, NFATc1-mCherry* ESCs were used to generate a mouse line. A whole mount of an embryonic day 9.5 (E9.5) *NFATc1-mCherry* mouse revealed the endocardial-specific expression of the mCherry reporter using fluorescent microscopy (Fig. 2.8B). Sections of the E9.5 heart confirmed expression of the *NFATc1-mCherry* transgene was restricted to the endocardial lining of the outflow tract and the AVC (Fig. 2.8C). Therefore, the *NFATc1-mCherry* transgene faithfully recapitulates the endogenous expression of NFATc1 within endocardial cells of the heart *in vivo* and serves as a great developmental tool for identifying and isolating endocardial cells *in vitro*.

After validating the expression of the *NFATc1-mCherry* transgene *in vivo*, we next sought to utilize the transgene to segregate endocardial and endothelial cells from differentiated *NFATc1-mCherry* ESCs. IF analysis of D8 EBs from *NFATc1-mCherry* ESCs that were differentiated using the hanging drop method verified the distinct expression of mCherry in endocardial cells that were separate from the remaining $CD31^+$ endothelium and $cTnT^+$ myocardium (Fig. 2.8D). After validating the endocardial-

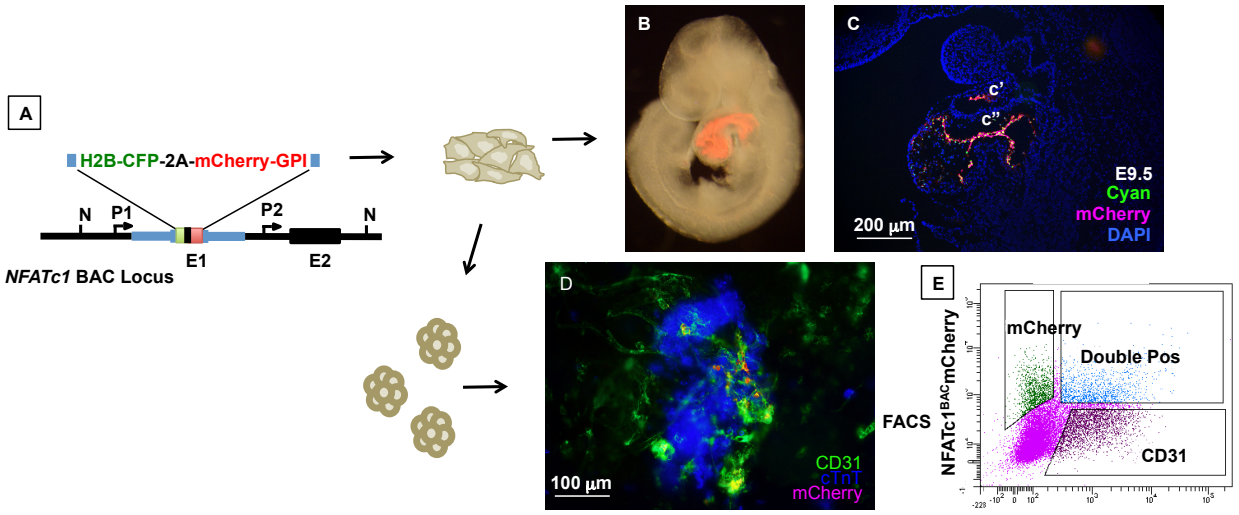

p-value	Fold Change	ID
1.30E-03	1.517	Tgfβ1
5.00E-05	2.060	Bmp2
5.00E-05	3.553	Fgf3
5.00E-05	4.770	Igf1
1.00E-04	2.464	Pdgfb

Figure 2.8. RNAseq identifies accentuated expression of growth factors in the endocardium. (A) The *NFATc1-mCherry* transgene contains a nuclear Cyan reporter and a membrane-linked mCherry reporter that is driven by *NFATc1* regulatory elements. Mouse ESCs consisting of the *NFATc1-mCherry* transgene was used to generate transgenic mice. (B) Whole mount immunofluorescence of an E9.5 embryo demonstrates the endocardial-restricted expression of mCherry in the developing heart. (C) A sagittal section of an E9.5 *NFATc1-mCherry* embryo reveals the nuclear Cyan and a membrane-anchored mCherry reporter within endocardial cells that line the OFT (c') and the AVC (c''). (D) Immunofluorescence of D8 *NFATc1-mCherry* EBs confirmed expression of the NFATc1-driven mCherry reporter in a subpopulation of $CD31^{+}$ endothelial cells located in close proximity to $cTnT^{+}$ myocardial cells. (E) Endocardial and endothelial cells were dissociated from D8 *NFATc1-mCherry* EBs and sorted according to their expression of mCherry and/or CD31. (F) Analysis of the RNAseq performed on the sorted cells revealed *Tgfb1*, *Bmp2*, *Fgf3*, *Igf1*, and *Pdgfb* were highly expressed in endocardial cells relative to the remaining population of endothelial cells according to a fold change of 1.5 or higher. (G) A

graph was generated to illustrate the differential expression analysis of *Tgfb1*, *Bmp2*, *Fgf3*, *Igf1*, and *Pdgfb* in endocardial cells compared to endothelial cells in counts per million (cpm).

specific expression of the *NFATc1-mCherry* transgene *in vitro*, endocardial cells ($mCherry^{+}/CD31^{+}$) and endothelial cells ($mCherry^{-}/CD31^{+}$) were dissociated from D8 *NFATc1-mCherry* EBs and isolated using fluorescence-activated cell sorting (FACS) (Fig. 2.8E). RNA-seq performed on the isolated endocardial cells compared to endothelial cells revealed several differences in their genetic profile. Among these differences was the expression of growth factors highly expressed in endocardial cells relative to endothelial cells, which included Tgfβ1, Bmp2, Fgf3, Igf1, and Pdgfb (Fig. 2.8F, G).

Before testing the potential of these growth factors in rescue experiments we first established that the expression of Bmp2, Fgf3, Igf1, Pdgfb, and Tgfβ1 was decreased in *NFATc1-DTR* EBs treated with DT from D4 to D8 of differentiation compared to untreated EBs (Fig. 2.9A). Given the roles these potential candidates have been reported to play during heart development, we proceeded to singly introduce Bmp2, Fgf3, Igf1, Pdgfb, and Tgfβ1 during endocardial ablation in an attempt to rescue myocardial differentiation and maturation (Engelmann et al., 1992, Van den Akker et al., 2008, Li et al., 2011, Urness et al., 2011, Papoutsi et al., 2018). Among the six growth factors analyzed, the addition of Bmp2 displayed the most potential for increasing the number of contracting D10 *NFATc1-DTR* EBs treated with DT from D4 to D8 relative to untreated EBs (Fig. 2.9B). This increase was not detected in *NFATc1-DTR* EBs treated with Bmp2 (in the absence of DT) from D4 to D8 compared to untreated EBs (Fig. 2.9C). Bmp2 treatment during endocardial ablation also resulted in the increased expression of myocyte differentiation markers *Nkx2.5*, *Isl1*, *Gata4*, *Gata6*, and *Hand2* in EBs treated with DT from D4 to D8 compared to EBs only treated with DT (Fig. 2.9D). Furthermore, the expression of late myocyte maturation markers *cTnT*, *αMHC*, *Mlc2a*, *Mlc2v*, and *HCN4* also increased in response to Bmp2 treatment during endocardial ablation (Fig. 2.9E). Altogether, these results suggest that during a critical

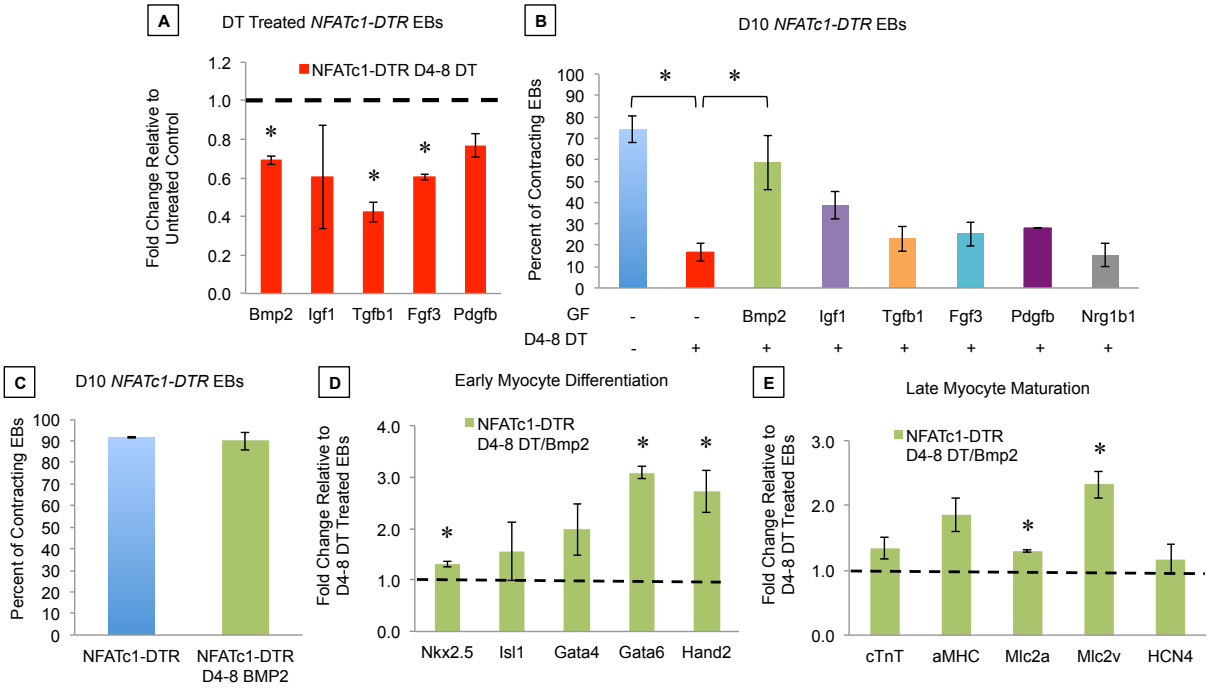

Figure 2.9. Bmp2 treatment partially rescues the differentiation and maturation of myocardial cells during endocardial ablation.

(A) The expression of growth factors *Bmp2*, *Ifg1*, *Tgfb1, Fgf3*, and *Pdgfb* was greatly attenuated in *NFATc1-DTR* EBs treated from D4 to D8 of differentiation compared to untreated EBs. (B) Among the growth factors added to *NFATc1-DTR* EBs during endocardial ablation between D4 and D8 of differentiation, Bmp2 displayed the greatest potential for increasing the percent of beating in D10 EBs. (C) The addition of Bmp2 to untreated *NFATc1-DTR* EBs from D4 to D8 of differentiation did not elicit any significant changes to the percent of beating on D10 of differentiation compared to control EBs. Bmp2 treatment during endocardial ablation from D4 to D8 of differentiation also increased the expression of (D) early and (E) late myocardial markers on D10 of differentiation relative to EBs that were only treated with DT.

developmental window, Bmp2 has the potential to partially restore the effects of endocardial ablation on the differentiation and maturation of myocardial cells by positively manipulating normal myocardial gene expression pathways.

The Addition of Bmp2 Increases the Quantity of Cardiomyocytes Present During Endocardial Ablation

To determine whether the partial restoration of cardiomyocyte gene expression and function detected during Bmp2 treatment was the result of an increase in cardiomyocytes present during endocardial ablation we investigated changes in proliferation. Bmp2 treatment during endocardial ablation from D4 to D6 of differentiation increased the number of MHC^+ cells present within D6 *NFATc1-DTR* EBs compared to those only treated with DT (Fig. 2.10A, B). However, quantification of $pHH3^+/MHC^+$ cells revealed that the increase in cardiomyocytes present in the absence of endocardial cells as a result of Bmp2 treatment was not due to a substantial increase in proliferation (Fig. 2.10C). Next, we considered the possibility that Bmp2 treatment decreased the number of cardiomyocytes undergoing cell death. In an attempt to test this possibility, we used a TUNEL assay to analyze myocardial cell death within D4-6 DT-treated *NFATc1-DTR* EBs rescued with or without Bmp2. Results from the assay demonstrated that the number of myocytes undergoing cell death was similar among *NFATc1-DTR* EBs treated with DT (Fig. 2.10D) and *NFATc1-DTR* EBs simultaneously treated with DT and Bmp2 (Fig. 2.10E). This observation was validated by the quantification of dying cardiomyocytes ($MHC^+/TUNEL^+$) present in D6 EBs following endocardial ablation and Bmp2 rescue (Fig. 2.10F). Overall, these results demonstrate that Bmp2 treatment during endocardial ablation augments the number of cardiomyocytes present in *NFATc1-DTR* EBs at D6 of differentiation with little to no influence on the proliferation or survival of cardiomyocytes.

The Expression of NFATc1-DTR and NFATc1-Cre is Restricted to Endocardial Cells from the Onset of Differentiation in vivo

Taken together, the decrease in cardiogenic gene expression and functional myocytes as a result

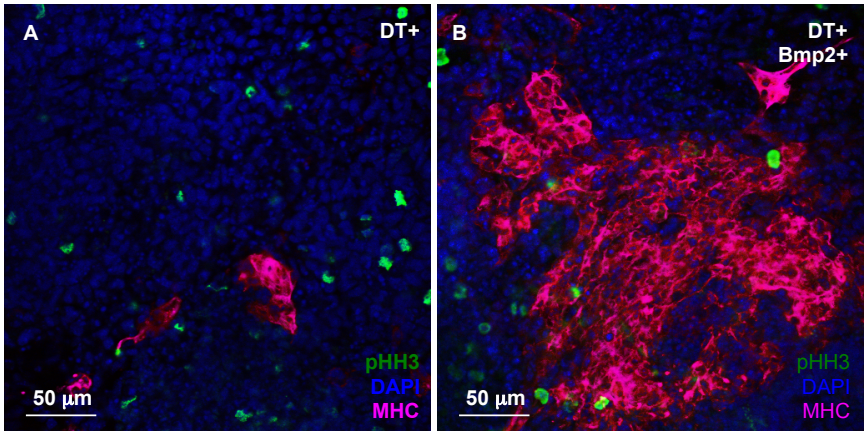
A
DT+
pHH3
DAPI
MHC
50 µm
B
DT+
Bmp2+
pHH3
DAPI
MHC
50 µm

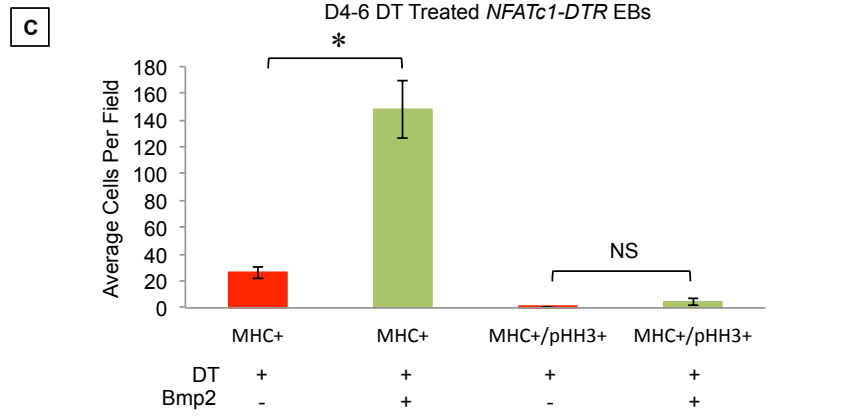
C
D4-6 DT Treated NFATc1-DTR EBs
Average Cells Per Field
180
160
140
120
100
80
60
40
20
0
*
NS
MHC+
MHC+
MHC+/pHH3+
MHC+/pHH3+
DT + + + +
Bmp2 - + - +

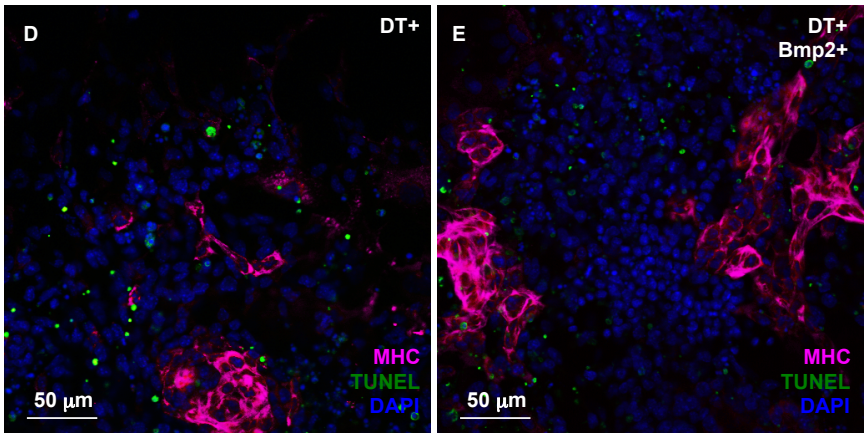
D
DT+
MHC
TUNEL
DAPI
50 µm
E
DT+
Bmp2+
MHC
TUNEL
DAPI
50 µm

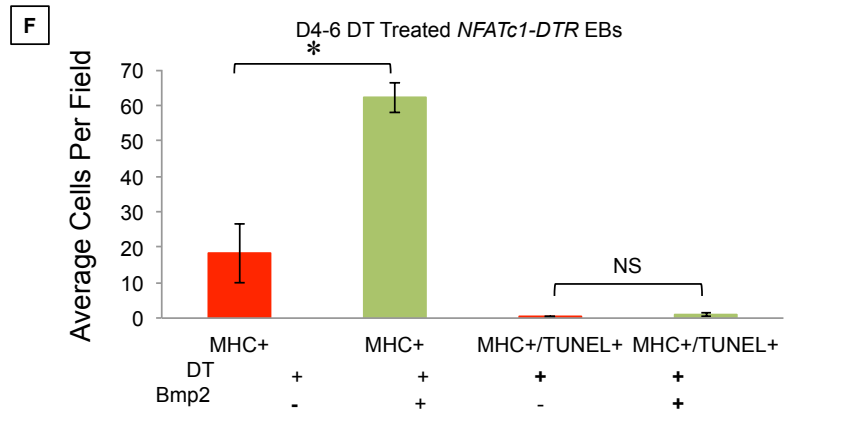
F
D4-6 DT Treated NFATc1-DTR EBs
Average Cells Per Field
70
60
50
40
30
20
10
0
*
NS
MHC+
MHC+
MHC+/TUNEL+
MHC+/TUNEL+
DT + + + +
Bmp2 - + - +

Figure 2.10. The addition of Bmp2 during endocardial ablation increases the number of cardiomyocytes detected in D6 *NFATc1-DTR* EBs.

Immunofluorescence was used to detect the presence of proliferating cardiomyocytes ($MHC^+/pHH3^+$) in *NFATc1-DTR* EBs treated with (A) DT alone and in those treated with (B) DT and Bmp2 from D4 to D6 of differentiation. (C) An assessment of $MHC^+/pHH3^+$ cells between the two groups revealed that the increase in number of cardiomyocytes present in *NFATc1-DTR* EBs as a result of Bmp2 treatment during endocardial ablation was not due to an increase in proliferation. TUNEL staining revealed a similar number of MHC^+ cardiomyocytes undergoing cell death in D6 *NFATc1-DTR* EBs treated with (D) DT from D4 to D6 and D6 *NFATc1-DTR* EBs treated with (E) DT and Bmp2 simultaneously from D4 to D6. (F) Quantification of $MHC^+/TUNEL^+$ cells revealed there was no difference in cell death among cardiomyocytes in DT-treated samples and Bmp2 rescue samples.

of endocardial ablation suggests that the myocardium requires an interaction with endocardial cells that involves Bmp signaling. However, these results could also be explained by the presence of multipotent cardiovascular progenitors that express NFATc1 and thus DTR. If this were so, then DT treatment would eradicate the progenitor population that normally give rise to both myocardial and endocardial cells and thus prevent the branching off of these respective lineages. To address and rule out the second explanation, we first analyzed the expression of the *NFATc1-DTR* transgene *in vivo* using a mouse line derived from *NFATc1-DTR* ESCs (Fig. 2.11A) (Poueymirou et al., 2007). Expression of the transgene GFP reporter was detected within endocardial cells that lined the outflow tract (OFT) (Fig. 2.11B) and atrioventricular canal (AVC) (Fig. 2.11C) of whole mount E9.5 *NFATc1-DTR* embryos (Zhou et al., 2005, Misfeldt et al., 2009). Furthermore, IF staining of an E9.5 *NFATc1-DTR* heart demonstrated the co-expression of the GFP reporter and endogenous NFATc1 within endocardial cells of the AVC (Fig. 2.11D-F). Additional IF analysis of an E9.5 *NFATc1-DTR* heart also revealed GFP expression emulates the spatial relationship between endocardial cells and cTnT+ myocardial cells previously reported (Fig. 2.11G) (Misfeldt et al., 2009). The expression of GFP was also restricted to endocardial cells lining the OFT and trabeculae of an E10.5 heart and the primitive valves of an E12.5 heart in whole mount *NFATc1-DTR* embryos (Fig. 2.11H-I) (Zhou et al., 2005, Misfeldt et al., 2009, Wu et al., 2011). Altogether, these results confirm that expression of the *NFATc1-DTR* transgene faithfully recapitulates the expression pattern of endogenous NFATc1 during heart development *in vivo*.

Although the *in vitro* and *in vivo* data presented in this study validates the endocardial-restricted expression of the *NFATc1-DTR* transgene, the lineage of *NFATc1-DTR*$^{+}$ cells remained unclear. To confirm that DT treatment only resulted in the ablation of endocardial cells and to exclude the likelihood that transcriptional regulatory elements of the *NFATc1* genomic locus within the BAC utilized to generate our *in vitro* and *in vitro* models induced the expression of DTR in additional cardiac progenitors and thus exclusively expressed in endocardial cells. Whole-mount X-gal staining of E10.0 embryos from a mating between *NFATc1-Cre* BAC and *Rosa26*^{LacZ} reporter mice demonstrated the expression of β- galactosidase (β-gal) primarily in endocardial cells of the heart (Fig. 2.12A-B). The endocardial- restricted expression

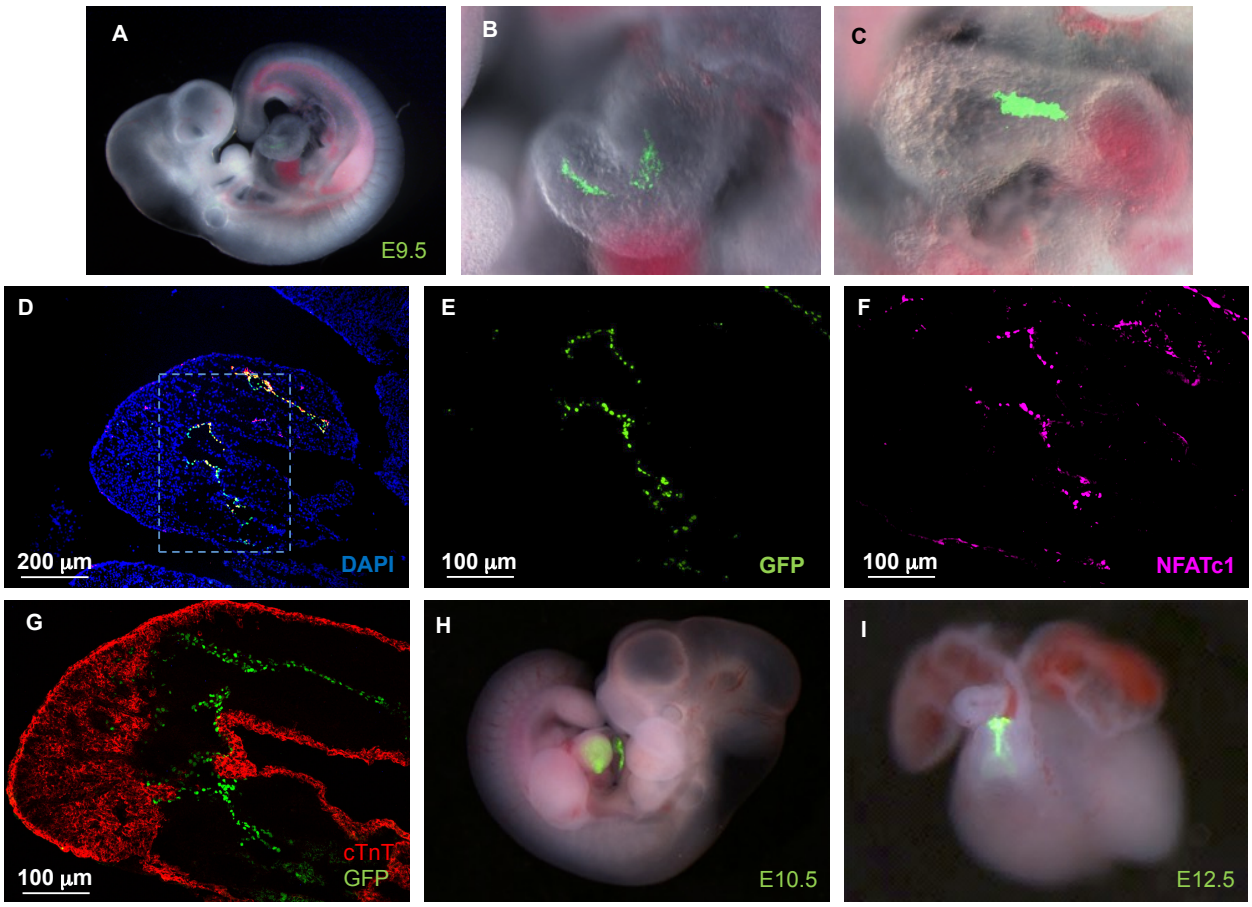

Figure 2.11. Expression of the *NFATc1-DTR* transgene is confined within endocardial cells of the developing heart *in vivo*.

(A) Fluorescent microscopy was used to detect expression of the GFP reporter within the heart of a whole mount E9.5 *NFATc1-DTR* embryo. The expression of GFP was restricted to the endocardial cells of the (B) OFT and the (C) AVC in the heart. Immunofluorescence of a sectioned (D) E9.5 heart demonstrated the expression of (E) GFP faithfully recapitulated (F) endogenous NFATc1 expression within endocardial cells. (G) GFP expression also coincided with the known location of endocardial cells relative to the $cTnT^{+}$ myocardium in an E9.5 heart. Expression of the *NFATc1-DTR* transgene can also be detected within the endocardial lining of the OFT and trabeculae in an (H) E10.5 heart and the valve primordium in an E12.5 heart.

result in their ablation, we used an *NFATc1-Cre* BAC transgenic mouse line in which Cre recombinase is of *NFATc1-Cre* was more evident following eosin staining of sectioned E10.0 *NFATc1-Cre; Rosa26*^{LacZ} embryos, which showed the location of β-gal^{+} endocardial cells lining the OFT (c') and the AVC (c'') (Fig. 2.12C). The expression of β-gal in mesenchymal cells of the endocardial cushion separating the left ventricular lumen (v) and the left atrium (a) was not surprising. This observation supports past studies that have reported a majority of the mesenchymal cells are derivatives of endocardial cells that upon suspending *NFATc1* expression underwent epithelial to mesenchymal transition (EMT) and migrated into the cardiac jelly during the initial stages of valvulogenesis (Wu et al., 2011). Therefore, the expression of β-gal within the cushions demarcates derivatives of NFATc1^{+} endocardial cells that contribute to the cardiac cushions (reviewed in (DeLaughter et al., 2011)). The presence of β−gal^{+} cells within the liver also supports past reports concerning the expression of *NFATc1* in other cell populations and further validates the fidelity of *NFATc1-Cre* expression (Zetterqvist et al., 2013). Overall, these results suggest that expression of the *NFATc1-Cre* transgene recapitulate endogenous *NFATc1* within a subpopulation of cells. Furthermore, Cre-mediated expression of *LacZ* in *NFATc1-Cre; Rosa26*^{LacZ} mice results in the delineation of all *NFATc1-Cre*$^{+}$ cells and their progeny.

To ensure expression of the *NFATc1-Cre* transgene is initiated at, and not prior to, the onset of endocardial specification, we investigated the time frame in which cells expressing endogenous NFATc1 were first identified in the developing heart (Misfeldt et al., 2009). X-gal staining of E7.75 *NFATc1-Cre; Rosa26*^{LacZ} embryos revealed β-gal expression within the cardiac crescent, which has been reported to encompass endocardial cells (Fig. 2.12D, E) (Misfeldt et al., 2009). Further investigation demonstrated the distinct position of β-gal^{+} endocardial cells within the cardiac primordium of a sectioned E7.75 *NFATc1-Cre; Rosa26*^{LacZ} embryo (Fig. 2.12F). Taken together, the data show that expression of *NFATc1-Cre* is restricted to endocardial cells *in vivo*, which are in agreement with the other NFATc1 BAC transgenic models analyzed in this study. The lineage tracing results of *NFATc1-Cre* expression validates that the *NFATc1* promoter of the transgene is not active within progenitor cells that give rise to

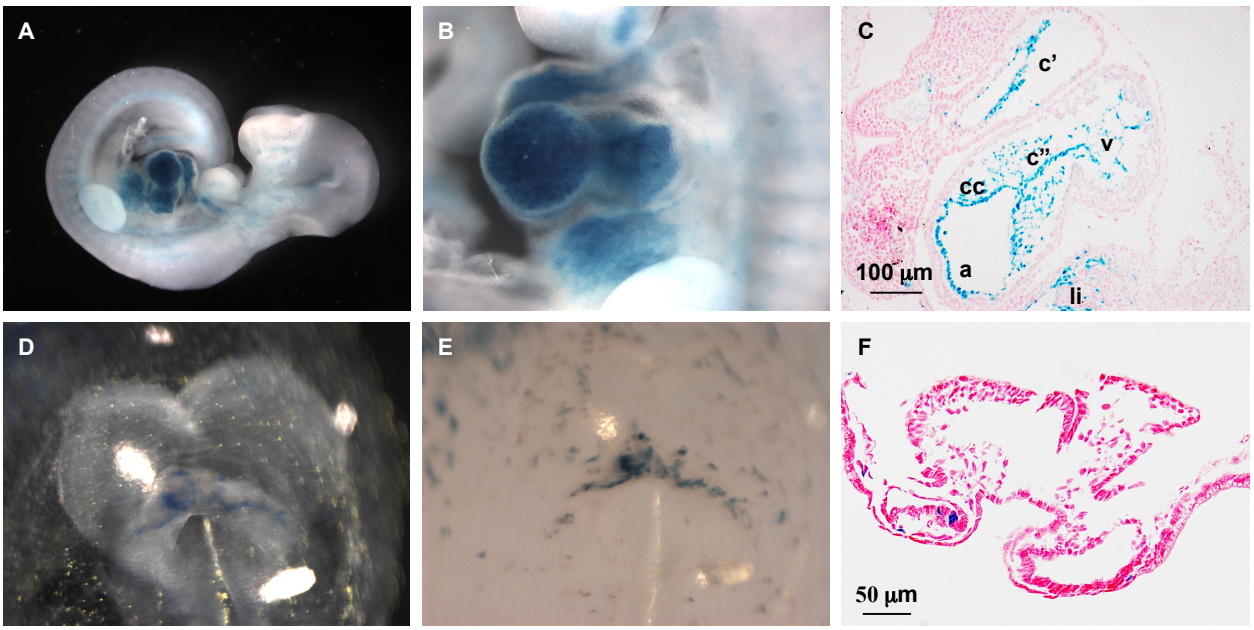

Figure 2.12. The *NFATc1-Cre* BAC transgene is specifically expressed in endocardial cells and their progeny.

(A, B) The overnight incubation of E10.0 *NFATc1-Cre*; *Rosa26*^{LacZ} embryos revealed the presence of β-gal^{+} cells within the heart. (C) Section of an E10.0 *NFATc1-Cre*; *Rosa26*^{LacZ} heart confirmed the expression of β-gal was restricted to the endocardial lining of the OFT (c') and the AVC (c''). The expression of β-gal was also detected in the mesenchyme of the cardiac cushion (cc) as well as the liver (li). (D, E) β-gal^{+} cells were localized within the cardiac crescent of an E7.75 *NFATc1-Cre; Rosa26*^{LacZ} embryo. (F) The expression of β-gal was detected within the cardiac primordium of a sectioned E7.75 *NFATc1-Cre BAC; Rosa26*^{LacZ} embryo. Atria, a; Ventricle, v.

myocardial cells. Given similar promoter elements were used in the *NFATc1-Cre* transgene as the *NFATc1- DTR* transgene, these results further supports the specificity of the endocardial ablation strategy utilized during cardiogenesis *in vitro*. The expression of DTR in *NFATc1-DTR* EBs is restricted to endocardial cells and not expressed in myocardial cells throughout cardiac differentiation. Therefore, the demise mediated by the presence of DT is limited to endocardial cells and excludes cardiomyocytes. Consequently, the decrease in myocardial differentiation, maturation, function, and cell number is the direct result of an attenuated population of endocardial cells.

D. Discussion

To date, there have been numerous studies on the essential interactions that occur between endocardial and myocardial cells during heart development from mid to late gestation. However, it is unknown whether such critical interactions occur during the initial stages of cardiogenesis. By taking advantage of the regulatory elements of the *NFATc1* locus and diphtheria toxin-mediated cell death via the diphtheria toxin receptor/diphtheria toxin ablation system we have generated a novel *in vitro* model that has allowed us to address this gap in the literature. Findings from this study provide evidence of an interaction between endocardial and myocardial cells within a specific period of cardiogenesis that is critical for the differentiation and maturation of the myocardium *in vitro*.

The time frame in which myocardial cells are dependent on the presence of endocardial cells during *in vitro* differentiation coincides with the expression of markers that delineate the onset of cardiogenesis such as *Nkx2.5*, *Mef2c*, and *Isl1*. Though expression of these markers is not required for the initiation of cardiomyogenesis, development of the primitive heart in murine embryos was compromised in their absence (Lyons et al., 1995, Lin et al., 1997, Cai et al., 2003, Prall et al., 2007, Li et al., 2016). The initiation of *βMHC* expression, a late cardiac sarcomere marker, was also shown to occur within the critical window of endocardial-myocardial interactions. Intriguingly, expression of both early and late myocyte differentiation markers was reduced significantly during endocardial ablation. Thus, the

presence of the endocardium is required during the same time at least a subset of myocardial cells are undergoing specification and determination.

Results from this study suggest that myocardial differentiation is dependent upon interactions with the endocardium that involve Bmp signaling during the early stage of cardiogenesis. These results are contrary to those reported by Palencia-Desai *et al.* which revealed Bmp signaling is critical for endocardial but not myocardial differentiation (Palencia-Desai et al., 2015). Following the genetic and chemical disruption of Bmp signaling at the tailbud stage of the zebrafish model system, myocardial development was minimally affected whereas the endocardium failed to differentiate according to the absence of *nfatc1* expression. A similar defect in endocardial differentiation detected in *hand2* zebrafish mutants deficient in myocardial progenitors was rescued by heat-shock-induced expression of *bmp2b*. Altogether, these results suggest the myocardium develops independently of Bmp signaling. Furthermore, the myocardium utilizes Bmp signaling to promote endocardial differentiation. The incongruity between results reported by Palencia-Desai *et al*. and our observations may be the result of species variability given that Bmp signaling has been reported to play a role in myocardial differentiation during the initial stages of myocardiogenesis in mouse, chicken, and human (Schlange et al., 2000, Kattman et al., 2011). For example, Bmp2 has been shown to elicit the expression of early cardiac transcription factors *Nkx2.5* and *Gata4* ectopically when produced by cells implanted in cultured, gastrulating chick embryos (Andrée et al., 1998). Past studies have also identified SMAD binding consensus sequences within the *Nkx2.5* regulatory element in mice, suggesting a role for BMP-mediated SMAD activity within the heart forming region during early cardiogenesis (Liberatore et al., 2002, Lien et al., 2002). Deletion in one of these sequences resulted in the absence of *Nkx2.5*-driven LacZ expression within the cardiac crescent as well as the myocardium of the OFT. Interestingly, the activating region (AR) 2 enhancer of *Nkx2.5* that consisted of SMAD and Nkx2.5 binding sites was found to be highly conserved in mouse, chicken, and human (Lien et al., 2002). The requirement for BMP signaling within a specific time frame to promote myocardiogenesis has also been reported in the *ex ovo* model system. Schlange *et al.* demonstrated that the addition of Noggin to explants of HH stage 4 chick embryos for 24 hours inhibited the expression of

Nkx2.5, Gata4, and ventricular MHC shortly after myocardial precursors have migrated through the primitive streak and prior to the formation of the bilateral cardiogenic regions (Schlange et al., 2000).

Multiple *in vitro* studies have enhanced the cardiogenic capacity of ESCs to generate an efficient number of functional cardiomyocytes through specific methods. One method includes the addition of BMP inhibitors within a set time frame of differentiation. The addition of Noggin prior to and during the initial days of *in vitro* differentiation has been found to promote myocardiogenesis at the expense of mesoderm-derived hematopoietic lineages, which recapitulate the regulatory role played by the ectoderm *in vivo* (Snyder et al., 2004, Yuasa et al., 2005, Lindsley et al., 2006, Misfeldt et al., 2009). GREMLIN2 (GREM2), another Bmp antagonist, has also been used to increase the output of cardiomyocytes *in vitro*. Grem2 treatment was reported to promote the differentiation of mature and functional atrial cardiomyocytes from mouse ESCs via noncanonical Bmp signaling and activation of the c-Jun N-terminal Kinase (JNK) signaling pathway (Tanwar et al., 2014). Recently, GREM2 was also found to promote the differentiation and proliferation of cardiac progenitor cells from differentiated human-induced pluripotent stem cells (hiPSCs) (Bylund et al., 2017). Interestingly, the initial expression of *GREM2* is concurrent with the specification of cardiac mesoderm and the expression of early myocyte markers *NKX2.5* and *ISL1* in differentiated hiPSCs. A similar expression pattern was observed in differentiated mouse ESCs, though detectable transcripts of *Nkx2.5* appeared to precede those of *Grem2*, temporally (Tanwar et al., 2014). Thus, it appears that Grem2 plays a role in the differentiation and proliferation of cardiomyocytes during early cardiogenesis. Findings from our study suggest a similar, time-sensitive window in which myocardial precursors require the activation of BMP signaling to differentiate into mature, contractile cardiomyocytes *in vitro*. It is possible that these seemingly conflicting results reflect a delicate level of Bmp signaling that is 1) required prior to and during myocardial differentiation and 2) established by a balance between the activation and inhibition of either the noncanonical or canonical Bmp signaling pathway, or both. This explanation is supported by the increased expression of *Grem2* observed in *NFATc1-DTR* EBs that were treated with both DT and Bmp2 (data not shown). Given that we did not detect a difference in the number of proliferating cardiomyocytes as a result of endocardial ablation nor

following rescue with Bmp2 treatment in *NFATc1-DTR* EBs, it is also possible that Bmp signaling is required for one facet of myocardial differentiation while Grem2, which was reported to promote proliferation, is required for another.

Though the consequences of endocardial ablation on the differentiation and maturation of myocardial cells were partially restored by the addition of Bmp2 in *NFATc1-DTR* EBs, the source of this growth factor under normal conditions is unknown. To date, there have been multiple studies on the role of Bmp secreted by the myocardium during certain morphogenetic events of cardiogenesis. Myocardial cells have been reported to secrete Bmp2 during heart development to induce endocardial EMT and development of the AVC during valvulogenesis. In one study, the endocardial cushion failed to form as a result of Bmp2 inhibition specifically in the atrioventricular myocardium or interruption of the Bmp type 1A receptor, *Bmpr1a*, in endocardial cells (Ma et al., 2005). Most recently, there has been an effort to elucidate the role of Bmp2 expression by endocardial cells. Saxon *et al.* revealed that endocardial-specific Bmp2 promotes the elongation, remodeling, and maturation of the atrioventricular endocardial cushion into AV valves and the ventricular septum (Saxon et al., 2017). Thus, there are at least two plausible explanations for the partial restoration of cardiomyocyte differentiation during endocardial ablation. One possible explanation is that myocardial cells are prompted to secrete Bmp2 via paracrine signaling from endocardial cells, which acts in an autoregulatory loop to induce and maintain the differentiation of myocardial precursors. Another possibility is that endocardial cells secrete Bmp2, which signal through Bmp receptors of cardiomyocyte progenitors to promote their differentiation and maturation. Further investigation will be required to define the mechanism of this critical cell-cell interaction.

CHAPTER III

CONCLUSIONS AND FUTURE DIRECTIONS

Endocardial-myocardial interactions have been reported to be essential for valvulogenesis, and trabeculation, and the formation of coronary vessels. Though we have acquired valuable information regarding the roles of endocardial and myocardial cells during these developmental processes, our knowledge only encompasses what occurs during the second half of gestation, after the heart tube has formed and looped. Given the shared origin of endocardial and myocardial cells from a mesoderm-derived population of multipotent cardiovascular progenitors and the persistent propinquity of these two cell types throughout heart development, we postulated that this spatial relationship is necessary for differentiation through cell-cell signaling. The purpose of this study was to ascertain interactions between endocardial and myocardial cells that influence myocardial differentiation during the early stages of cardiogenesis. By ablating endocardial cells throughout a ten-day span of *in vitro* differentiation, we were able to identify a critical interaction between endocardial and myocardial cells. With further investigation, we determined that myocardial differentiation is reliant on signaling from the endocardium within the same time frame expression of early myocyte markers is first detected *in vitro*. Given the temporal expression of these markers is reduced at the onset of cardiogenesis, we hypothesize that the earliest endocardial-myocardial interaction required for myocardial differentiation occurs at the cardiac crescent stage when the juxtaposition of myocardial and endocardial progenitors is initially observed *in vivo* (Kattman et al., 2006, Moretti et al., 2006, Bondue et al., 2011, Lescroart et al., 2014, Tyser et al., 2016).

Though results from our study show Bmp signaling is involved in early endocardial-myocardial interactions, the mechanism regarding how this signaling pathway is important remains unclear. Shortly after specification, it is possible that pro-cardiomyocytes depend on Bmp signaling through interactions with endocardial cells to continue differentiating into mature, contractile units. As a result of this dependence, ablating endocardial cells could cause pro-cardiomyocytes to enter a state of quiescence as they await the factors necessary for differentiation, such as Bmp. This could explain why we detected an

increase in the number of functional cardiomyocytes as well as in the expression of myocyte markers when Bmp2 was introduced to *NFATc1-DTR* EBs in culture during endocardial ablation. To test this possibility, we can stain *NFATc1-DTR* EBs treated with or without Bmp2 during endocardial ablation at D5, D6, D7, or D8 for markers of quiescent Nkx2.5+ cardiac progenitor cells. Potentially, results from the staining will reveal a decrease in the number of quiescent Nkx2.5+ cardiac progenitor cells in *NFATc1-DTR* EBs following Bmp2 treatment. Delaying Bmp2 treatment of NFATc1-DTR EBs in culture until after endocardial ablation can also test the possibility of pro-cardiomyocytes entering a quiescent state. If the pro-cardiomyocytes are truly present and awaiting Bmp signaling to differentiate, then we will continue to observe an increase in the presence of contracting myocytes, though maybe not to the same extent given the time sensitivity of endocardial-myocardial interactions during the early stage of cardiogenesis.

In summary, the endocardium plays an essential role in the differentiation of myocardial cells from the onset of cardiogenesis. Most importantly, interactions between endocardial and myocardial cells are not restricted to one time frame but occur continually throughout embryogenesis to promote proliferation, a series of morphological changes, and vascularization in the heart. Thus, it is important to consider the endocardium when devising future stem cell based replacement therapies with cardiogenic potential and the proficiency of yielding a significant number of functional cardiomyocytes (Pasquier et al., 2017, Zhang et al., 2018).

REFERENCES

ABU-ISSA, R., KIRBY, M.L. 2007. Heart field: from mesoderm to heart tube. *Annu Rev Cell Dev Biol.,* 23**,** 45-68.

ANDRÉE, B., DUPREZ, D., VORBUSCH, B., ARNOLD, H.H., BRAND, T. 1998. BMP-2 induces ectopic expression of cardiac lineage markers and interferes with somite formation in chicken embryos. *Mech Dev.,* 70**,** 119-31.

BALDWIN, H. S., SHEN, H.M., YAN, H.C., DELISSER, H.M., CHUNG, A., MICKANIN, C., TRASK, T., KIRSCHBAUM, N.E., NEWMAN, P.J., ALBELDA, S.M., 1994. Platelet endothelial cell adhesion molecule-1 (PECAM-1/CD31): alternatively spliced, functionally distinct isoforms expressed during mammalian cardiovascular development. *Development. ,* 120**,** 2539-2553.

BOHELER, K. R., CZYZ, J., TWEEDIE, D., YANG, H.T., ANISIMOV, S.V., WOBUS, A.M. 2002. Differentiation of pluripotent embryonic stem cells into cardiomyocytes. *Circ Res.,* 91**,** 189-201.

BONDUE, A., TÄNNLER, S., CHIAPPARO, G., CHABAB, S., RAMIALISON, M., PAULISSEN, C., BECK, B., HARVEY, R., BLANPAIN ,C. 2011. Defining the earliest step of cardiovascular progenitor specification during embryonic stem cell differentiation. *J Cell Biol.,* 192**,** 751-65.

BROWN, C. B., BALDWIN, H.S. 2006. Neural crest contribution to the cardiovascular system. *Adv Exp Med Biol. ,* 589**,** 134-54.

BU, L., JIANG, X., MARTIN-PUIG, S., CARON, L., ZHU, S., SHAO, Y., ROBERTS, D.J., HUANG, P.L., DOMIAN, I.J., CHIEN, K.R. 2009. Human ISL1 heart progenitors generate diverse multipotent cardiovascular cell lineages. *Nature.,* 460**,** 113–117.

BUCKINGHAM, M., MEILHAC, S., ZAFFRAN, S. 2005. Building the mammalian heart from two sources of myocardial cells. *Nat Rev Genet.,* 6**,** 826-835.

BUSSMANN, J., BAKKERS, J., SCHULTE-MERKER, S. 2007. Early endocardial morphogenesis requires Scl/Tal1. *PLoS Genet.,* 3**,** e140.

BYLUND, J. B., TRINH, L.T., AWGULEWITSCH, C.P., PAIK, D.T., JETTER, C., JHA, R., ZHANG, J., NOLAN, K., XU, C., THOMPSON, T.B., KAMP, T.J., HATZOPOULOS, A.K.1. 2017. Coordinated Proliferation and Differentiation of Human-Induced Pluripotent Stem Cell-Derived Cardiac Progenitor Cells Depend on Bone Morphogenetic Protein Signaling Regulation by GREMLIN 2. *Stem Cells Dev.,* 26**,** 678-693.

CAI, C. L., LIANG, X., SHI, Y., CHU, P.H., PFAFF, S.L., CHEN, J., EVANS, S. 2003. Isl1 identifies a cardiac progenitor population that proliferates prior to differentiation and contributes a majority of cells to the heart. *Dev Cell.,* 5**,** 877–889.

CHAKRABORTY, S., COMBS, M.D., YUTZEY, K.E. 2010. Transcriptional regulation of heart valve progenitor cells. *Pediatr Cardiol. ,* 31**,** 414-421.

CHANG, C. P., NEILSON, J.R., BAYLE, J.H., GESTWICKI, J.E., KUO, A., STANKUNAS, K., GRAEF, I.A., CRABTREE, G.R. 2004. A field of myocardial-endocardial NFAT signaling underlies heart valve morphogenesis. *Cell.,* 118**,** 649-663.

CHEN, H., ZHANG, W., SUN, X., YOSHIMOTO, M., CHEN, Z., ZHU, W., LIU, J., SHEN, Y., YONG, W., LI, D., ZHANG, J., LIN, Y., LI, B., VANDUSEN, N.J., SNIDER, P., SCHWARTZ, R.J., CONWAY, S.J., FIELD, L.J., YODER, M.C., FIRULLI, A.B., CARLESSO, N., TOWBIN, J.A., SHOU, W. 2013. Fkbp1a controls ventricular myocardium trabeculation and compaction by regulating endocardial Notch1 activity. *Development.,* 140**,** 1946-1957.

CHRISTOFOROU, N., MILLER, R.A., HILL, C.M., JIE, C.C., MCCALLION, A.S., GEARHART, J.D. 2008. Mouse ES cell-derived cardiac precursor cells are multipotent and facilitate identification of novel cardiac genes. *J Clin Invest.,* 118**,** 894-903.

COFFIN, J. D., POOLE, T.J. 1988. Embryonic vascular development: immunohistochemical identification of the origin and subsequent morphogenesis of the major vessel primordia in quail embryos. *Development.,* 102**,** 735-48.

COFFIN, J. D., POOLE, T.J. 1991. Endothelial cell origin and migration in embryonic heart and cranial blood vessel development. *Anat Rec. ,* 231**,** 383-95.

COHEN-GOULD, L., MIKAWA, T. 1996. The fate diversity of mesodermal cells within the heart field during chicken early embryogenesis. *Dev Biol.,* 177**,** 265-273.

DE LA POMPA, J. L., TIMMERMAN, L.A., TAKIMOTO, H., YOSHIDA, H., ELIA, A.J., SAMPER, E., POTTER, J., WAKEHAM, A., MARENGERE, L., LANGILLE, B.L., CRABTREE, G.R., MAK, T.W. 1998. Role of the NF-ATc transcription factor in morphogenesis of cardiac valves and septum. *Nature.,* 392**,** 182-186.

DELAUGHTER, D. M., BICK, A.G., WAKIMOTO, H., MCKEAN, D., GORHAM, J.M., KATHIRIYA, I.S., HINSON, J.T., HOMSY, J., GRAY, J., PU, W., BRUNEAU, B.G., SEIDMAN, J.G., SEIDMAN, C. E. 2016. Single-Cell Resolution of Temporal Gene Expression during Heart Development. *Dev Cell.,* 39**,** 480-490.

DELAUGHTER, D. M., SAINT-JEAN, L., BALDWIN, H.S., BARNETT, J.V. 2011. What chick and mouse models have taught us about the role of the endocardium in congenital heart disease. *Birth Defects Res A Clin Mol Teratol.,* 91**,** 511-525.

DONNELLY, M. L., LUKE, G., MEHROTRA, A., LI, X., HUGHES, L.E., GANI, D., RYAN, M.D., 2001. Analysis of the aphthovirus 2A/2B polyprotein 'cleavage' mechanism indicates not a proteolytic reaction, but a novel translational effect: a putative ribosomal 'skip'. *J Gen Virol.,* 82**,** 1013-25.

EISENBERG, C. A., BADER, D. 1995a. QCE-6: A Clonal Cell Line with Cardiac Myogenic and Endothelial Cell Potentials. *Dev Biol.,* 167**,** 469–481.

EISENBERG, L. M., MARKWALD, R.R. 1995b. Molecular regulation of atrioventricular valvuloseptal morphogenesis. *Circ Res.,* 77**,** 1-6.

EMA, M., TAKAHASHI, S., ROSSANT, J. 2006. Deletion of the selection cassette, but not cis-acting elements, in targeted Flk1-lacZ allele reveals Flk1 expression in multipotent mesodermal progenitors. *Blood.,* 107**,** 111-117.

ENGELMANN, G. L., BOEHM, K.D., BIRCHENALL-ROBERTS, M.C., RUSCETTI, F.W. 1992. Transforming growth factor-beta 1 in heart development. *Mech Dev.,* 38**,** 85-97.

GASSMANN, M., CASAGRANDA, F., ORIOLI, D., SIMON, H., LAI, C., KLEIN, R., LEMKE, G. 1995. Aberrant neural and cardiac development in mice lacking the ErbB4 neuregulin receptor. *Nature.,* 378**,** 390-394.

GEORGE, S. H., GERTSENSTEIN, M., VINTERSTEN, K., KORETS-SMITH, E., MURPHY, J., STEVENS, M.E., HAIGH, J.J., NAGY, A. 2007. Developmental and adult phenotyping directly from mutant embryonic stem cells. *Proc Natl Acad Sci U S A.,* 104**,** 4455-60.

GREGO-BESSA, J., LUNA-ZURITA, L., DEL MONTE, G., BOLÓS, V., MELGAR, P., ARANDILLA, A., GARRATT, A.N., ZANG, H., MUKOUYAMA, Y.S., CHEN, H., SHOU, W., BALLESTAR, E., ESTELLER, M., ROJAS, A., PÉREZ-POMARES, J.M., DE LA POMPA, J.L. 2007. Notch signaling is essential for ventricular chamber development. *Dev Cell.,* 12**,** 415-429.

HARRIS, I. S., BLACK, B. L. 2010. Development of the endocardium. *Pediatr Cardiol.,* 31**,** 391-9.

HIGH, F. A., EPSTEIN, J.A. 2008. The multifaceted role of Notch in cardiac development and disease. *Nat. Rev. Genet.,* 9**,** 49-61.

HS., B. 1996 Early embryonic vascular development. Cardiovascular Research*.,* 31**,** E34-45.

HUTSON, M. R., KIRBY, M.L. 2003. Neural crest and cardiovascular development: a 20-year perspective. *Birth Defects Res C Embryo Today. ,* 69**,** 2-13.

ISHII, Y., LANGBERG, J., ROSBOROUGH, K., MIKAWA, T. 2009. Endothelial cell lineages of the heart. *Cell Tissue Res.,* 335**,** 67-73.

IWAMOTO, R., MEKADA, E. 2006. ErbB and HB-EGF signaling in heart development and function. *Cell Struct Funct.,* 31**,** 1-14.

IWAMOTO, R., YAMAZAKI, S., ASAKURA, M., TAKASHIMA, S., HASUWA, H., MIYADO, K., ADACHI, S., KITAKAZE, M., HASHIMOTO, K., RAAB, G., NANBA, D., HIGASHIYAMA, S., HORI, M., KLAGSBRUN, M., MEKADA, E. 2003. Heparin-binding EGF-like growth factor and ErbB signaling is essential for heart function. *Proc Natl Acad Sci U S A.,* 100**,** 3221-3226.

KATTMAN, S. J., HUBER, T.L., KELLER, G.M., 2006. Multipotent flk-1+ cardiovascular progenitor cells give rise to the cardiomyocyte, endothelial, and vascular smooth muscle lineages. *Dev Cell.,* 11**,** 723-732.

KATTMAN, S. J., WITTY, A.D., GAGLIARDI, M., DUBOIS, N.C., NIAPOUR, M., HOTTA, A., ELLIS, J., KELLER, G. 2011. Stage-specific optimization of activin/nodal and BMP signaling promotes cardiac differentiation of mouse and human pluripotent stem cell lines. *Cell Stem Cell.,* 8**,** 228-40.

KIRBY, M. L., WALDO, K.L. 1995. Neural crest and cardiovascular patterning. *Circ Res.,* 77**,** 211-5.

KOUSKOFF, V., LACAUD, G., SCHWANTZ, S., FEHLING, H.J., KELLER, G. 2005. Sequential development of hematopoietic and cardiac mesoderm during embryonic stem cell differentiation. *Proc Natl Acad Sci U S A.,* 102**,** 13170-13175.

KUBALAK, S. W., MILLER-HANCE, W.C., O'BRIEN, T.X., DYSON, E., CHIEN, K.R. 1994. Chamber specification of atrial myosin light chain-2 expression precedes septation during murine cardiogenesis. *J Biol Chem.,* 269**,** 16961-70.

LEE, E. C., YU, D., MARTINEZ DE VELASCO, J., TESSAROLLO, L., SWING, D.A., COURT, D.L., JENKINS, N.A., COPELAND, N.G., 2001. A highly efficient Escherichia coli-based chromosome engineering system adapted for recombinogenic targeting and subcloning of BAC DNA. *Genomics.,* 73**,** 56-65.

LEE, K. F., SIMON, H., CHEN, H., BATES, B., HUNG, M.C., HAUSER, C. 1995. Requirement for neuregulin receptor erbB2 in neural and cardiac development. *Nature.,* 378**,** 394-398.

LEE, R. K., STAINIER, D.Y., WEINSTEIN, B.M., FISHMAN, M.C. 1994. Cardiovascular development in the zebrafish. II. Endocardial progenitors are sequestered within the heart field. *Development.,* 120**,** 3361-6.

LESCROART, F., CHABAB, S., LIN, X., RULANDS, S., PAULISSEN, C., RODOLOSSE, A., AUER, H., ACHOURI, Y., DUBOIS, C., BONDUE, A., SIMONS, B.D., BLANPAIN, C. 2014. Early lineage restriction in temporally distinct populations of Mesp1 progenitors during mammalian heart development. *Nat Cell Biol. ,* 16**,** 829-840. .

LI, G., XU, A., SIM, S., PRIEST, J.R., TIAN, X., KHAN, T., QUERTERMOUS, T., ZHOU, B., TSAO, P.S., QUAKE, S.R., WU, S.M. 2016. Transcriptomic Profiling Maps Anatomically Patterned Subpopulations among Single Embryonic Cardiac Cells. *Dev Cell.,* 39**,** 491-507.

LI, P., CAVALLERO, S., GU, Y., CHEN, T.H., HUGHES, J., HASSAN, A.B., BRÜNING, J.C., PASHMFOROUSH, M., SUCOV, H.M. 2011. IGF signaling directs ventricular cardiomyocyte proliferation during embryonic heart development. *Development.,* 138**,** 1795-805.

LIBERATORE, C. M., SEARCY-SCHRICK, R.D., VINCENT, E.B., YUTZEY, K.E. 2002. Nkx-2.5 gene induction in mice is mediated by a Smad consensus regulatory region. *Dev Biol.,* 244**,** 243-56.

LIEN, C. L., MCANALLY, J., RICHARDSON, J.A., OLSON, E.N. 2002. Cardiac-specific activity of an Nkx2-5 enhancer requires an evolutionarily conserved Smad binding site. *Dev Biol.,* 244**,** 257-66.

LIN, Q., SCHWARZ, J., BUCANA, C., OLSON, E.N. 1997. Control of mouse cardiac morphogenesis and myogenesis by transcription factor MEF2C. *Science.,* 276**,** 1404-7.

LINASK, K. K. 1992. N-cadherin localization in early heart development and polar expression of Na+,K(+)-ATPase, and integrin during pericardial coelom formation and epithelialization of the differentiating myocardium. *Dev Biol.,* 151**,** 213-24.

LINDSLEY, R. C., GILL, J.G., KYBA, M., MURPHY, T.L., MURPHY, K.M. 2006. Canonical Wnt signaling is required for development of embryonic stem cell-derived mesoderm. *Development.,* 133**,** 3787-96.

LYONS, G. E., SCHIAFFINO, S., SASSOON, D., BARTON, P., BUCKINGHAM, M. 1990. Developmental regulation of myosin gene expression in mouse cardiac muscle. *J Cell Biol.,* 111**,** 2427-36.

LYONS, I., PARSONS, L.M., HARTLEY, L., LI, R., ANDREWS, J.E., ROBB, L., HARVEY, R.P. 1995. Myogenic and morphogenetic defects in the heart tubes of murine embryos lacking the homeo box gene Nkx2-5. *Genes Dev.,* 9**,** 1654-66.

MA, L., LU, M.F., SCHWARTZ, R.J., MARTIN, J.F. 2005. Bmp2 is essential for cardiac cushion epithelial-mesenchymal transition and myocardial patterning. *Development.,* 132**,** 5601-11.

MASINO, A. M., GALLARDO, T.D., WILCOX, C.A., OLSON, E.N., WILLIAMS, R.S., GARRY, D.J. 2004. Transcriptional regulation of cardiac progenitor cell populations. . *Circ Res.,* 95**,** 389–397.

MEYER, D., BIRCHMEIER, C. 1995. Multiple essential functions of neuregulin in development. *Nature.,* 378**,** 386-390.

MILGROM-HOFFMAN, M., HARRELSON, Z., FERRARA, N., ZELZER, E., EVANS, S.M., TZAHOR, E. 2011. The heart endocardium is derived from vascular endothelial progenitors. *Development. ,* 138**,** 4777-4787.

MISFELDT, A. M., BOYLE, S.C., TOMPKINS, K.L., BAUTCH, V.L., LABOSKY, P.A., BALDWIN, H.S. 2009. Endocardial cells are a distinct endothelial lineage derived from Flk1+ multipotent cardiovascular progenitors. *Dev Biol.,* 333**,** 78-89.

MITAMURA, T., HIGASHIYAMA, S., TANIGUCHI, N., KLAGSBRUN, M., MEKADA, E., 1995. Diphtheria toxin binds to the epidermal growth factor (EGF)-like domain of human heparin-binding EGF-like growth factor/diphtheria toxin receptor and inhibits specifically its mitogenic activity. *J Biol Chem.,* 270**,** 1015-9.

MORETTI, A., CARON, L., NAKANO, A., LAM, J.T., BERNSHAUSEN, A., CHEN, Y., QYANG, Y., BU, L., SASAKI, M., MARTIN-PUIG, S., SUN, Y., EVANS, S.M., LAUGWITZ, K.L., CHIEN, K.R. 2006. Multipotent embryonic isl1+ progenitor cells lead to cardiac, smooth muscle, and endothelial cell diversification. *Cell.,* 127**,** 1151–1165.

MOTOIKE, T., MARKHAM, D.W., ROSSANT, J., SATO, T.N. 2003. Evidence for novel fate of Flk1+ progenitor: Contribution to muscle lineage. *Genesis.,* 35**,** 153–159.

NADEAU, M., GEORGES, R.O., LAFOREST, B., YAMAK, A., LEFEBVRE, C., BEAUREGARD, J., PARADIS, P., BRUNEAU, B.G., ANDELFINGER, G., NEMER, M. 2010. An endocardial pathway involving Tbx5, Gata4, and Nos3 required for atrial septum formation. *Proc Natl Acad Sci U S A.,* 107**,** 19356-19361.

O'BRIEN, T. X., LEE, K.J., CHIEN, K.R. 1993. Positional specification of ventricular myosin light chain 2 expression in the primitive murine heart tube. *Proc Natl Acad Sci U S A.,* 90**,** 5157-61.

ODIETE, O., HILL, M.F., SAWYER, D.B. 2012. Neuregulin in cardiovascular development and disease. *Circ Res.,* 111**,** 1376-1385.

PALENCIA-DESAI, S., ROST, M.S., SCHUMACHER, J.A., TON, Q.V., CRAIG, M.P., BALTRUNAITE, K., KOENIG, A.L., WANG, J., POSS, K.D., CHI, N.C., STAINIER, D.Y., SUMANAS, S. 2015. Myocardium and BMP signaling are required for endocardial differentiation. *Development.,* 142**,** 2304-2315.

PALPANT, N. J., PABON, L., ROBERTS, M., HADLAND, B., JONES, D., JONES, C., MOON, R.T., RUZZO, W.L., BERNSTEIN, I., ZHENG, Y., MURRY, C.E. 2015. Inhibition of β-catenin signaling respecifies anterior-like endothelium into beating human cardiomyocytes. *Development.,* 142**,** 3198-3209.

PAPOUTSI, T., LUNA-ZURITA, L., PRADOS, B., ZAFFRAN, S., DE LA POMPA, J.L. 2018 Bmp2 and Notch cooperate to pattern the embryonic endocardium. *Development.,* 145**,** dev163378.

PASQUIER, J., GUPTA, R., RIOULT, D., HOARAU-VÉCHOT, J., COURJARET, R., MACHACA, K., AL SUWAIDI, J., STANLEY, E.G., RAFII, S., ELLIOTT, D.A., ABI KHALIL, C., RAFII, A. 2017. Coculturing with endothelial cells promotes in vitro maturation and electrical coupling of human embryonic stem cell-derived cardiomyocytes. *J Heart Lung Transplant.,* 36**,** 684-693.

PENTASSUGLIA, L., SAWYER, D,B. 2009. The role of Neuregulin-1beta/ErbB signaling in the heart. *Exp. Cell Res.,* 315**,** 627-637.

POUEYMIROU, W. T., AUERBACH, W., FRENDEWEY, D., HICKEY, J.F., ESCARAVAGE, J.M., ESAU, L., DORÉ, A.T., STEVENS, S., ADAMS, N.C., DOMINGUEZ, M.G., GALE, N.W., YANCOPOULOS, G.D., DECHIARA, T.M., VALENZUELA, D.M., 2007. F0 generation mice fully derived from gene-targeted embryonic stem cells allowing immediate phenotypic analyses. *Nat Biotechnol.,* 25**,** 91-9.

PRALL, O. W., MENON, M.K., SOLLOWAY, M.J., WATANABE, Y., ZAFFRAN, S., BAJOLLE, F., BIBEN, C., MCBRIDE, J.J., ROBERTSON, B.R., CHAULET, H., STENNARD, F.A., WISE, N., SCHAFT, D., WOLSTEIN, O., FURTADO, M.B., SHIRATORI, H., CHIEN, K.R., HAMADA, H., BLACK, B.L., SAGA, Y., ROBERTSON, E.J., BUCKINGHAM, M.E., HARVEY, R.P. 2007. An Nkx2-5/Bmp2/Smad1 negative feedback loop controls heart progenitor specification and proliferation. *Cell.,* 128**,** 947-59.

PUCÉAT, M. 2013. Embryological origin of the endocardium and derived valve progenitor cells: From developmental biology to stem cell-based valve repair. *Biochim Biophys Acta.,* 1833**,** 917–922.

RANGER, A. M., GRUSBY, M.J., HODGE, M.R., GRAVALLESE, E.M., DE LA BROUSSE, F.C., HOEY, T., MICKANIN, C., BALDWIN, H.S., GLIMCHER, L.H. 1998. The transcription factor NF-ATc is essential for cardiac valve formation. *Nature.,* 392**,** 186-190.

SAXON, J. G., BAER, D.R., BARTON, J.A., HAWKINS, T., WU, B., TRUSK, T.C., HARRIS, S.E., ZHOU, B., MISHINA, Y., SUGI, Y., 2017. BMP2 expression in the endocardial lineage is required for AV endocardial cushion maturation and remodeling. *Dev Biol.,* 430**,** 113-128.

SCHLANGE, T., ANDRÉE, B., ARNOLD, H.H., BRAND, T. 2000. BMP2 is required for early heart development during a distinct time period. *Mech Dev.,* 91**,** 259-70.

SCHULZ, H., KOLDE, R., ADLER, P., AKSOY, I., ANASTASSIADIS, K., BADER, M., BILLON, N., BOEUF, H., BOURILLOT, P.Y., BUCHHOLZ, F., DANI, C., DOSS, M.X., FORRESTER, L., GITTON, M., HENRIQUE, D., HESCHELER, J., HIMMELBAUER, H., HÜBNER, N., KARANTZALI, E., KRETSOVALI, A., LUBITZ, S., PRADIER, L., RAI, M., REIMAND, J., ROLLETSCHEK, A., SACHINIDIS, A., SAVATIER, P., STEWART, F., STORM, M.P., TROUILLAS, M., VILO, J., WELHAM, M.J., WINKLER, J., WOBUS, A.M., HATZOPOULOS, A.K.; FUNCTIONAL GENOMICS IN EMBRYONIC STEM CELLS CONSORTIUM. 2009. The FunGenES database: a genomics resource for mouse embryonic stem cell differentiation. *PLoS One.,* 4**,** e6804.

SNYDER, A., FRASER, S.T., BARON, M.H. 2004. Bone morphogenetic proteins in vertebrate hematopoietic development. *J Cell Biochem.,* 93**,** 224-32.

SRIVASTAVA, D. 2006. Genetic regulation of cardiogenesis and congenital heart disease. *Annu Rev Pathol.***,** 199-213.

SRIVASTAVA, D., THOMAS, T., LIN, Q., KIRBY, M.L., BROWN, D., OLSON, E.N. 1997. Regulation of cardiac mesodermal and neural crest development by the bHLH transcription factor, dHAND. *Nat Genet.,* 16**,** 154-60.

STAINIER, D. Y., WEINSTEIN, B.M., DETRICH, H.W. 3RD., ZON, LI., FISHMAN, M.C. 1995. Cloche, an early acting zebrafish gene, is required by both the endothelial and hematopoietic lineages. *Development.,* 121**,** 3141-3150.

STEWART, M. D., JANG, C.W., HONG, N.W., AUSTIN, A.P., BEHRINGER, R.R. 2009. Dual fluorescent protein reporters for studying cell behaviors in vivo. *Genesis.,* 47**,** 708-17.

STOLLER, J. Z., EPSTEIN, J.A. 2005. Cardiac neural crest. *Semin Cell Dev Biol. ,* 16**,** 704-15.

SUGI, Y., MARKWALD, R.R. 1996. Formation and early morphogenesis of endocardial endothelial precursor cells and the role of endoderm. *Dev Biol.,* 175**,** 66-83.

SUGI, Y., MARKWALD, R.R. 2003. Endodermal growth factors promote endocardial precursor cell formation from precardiac mesoderm. *Dev Biol.,* 263**,** 35-49.

SUGI Y, M. R. 1996 Formation and early morphogenesis of endocardial endothelial precursor cells and the role of endoderm. Developmental Biology*.,* 175**,** 66-83.

TAM, P. P., PARAMESWARAN, M., KINDER, S.J., WEINBERGER, R.P. 1997. The allocation of epiblast cells to the embryonic heart and other mesodermal lineages: the role of ingression and tissue movement during gastrulation. *Development.,* 124**,** 1631-1642.

TANAKA, M., CHEN, Z., BARTUNKOVA, S., YAMASAKI, N., IZUMO, S. 1999. The cardiac homeobox gene Csx/Nkx2.5 lies genetically upstream of multiple genes essential for heart development. *Development. ,* 126**,** 1269-1280.

TANWAR, V., BYLUND, J.B., HU, J., YAN, J., WALTHALL, J.M., MUKHERJEE, A., HEATON, W.H., WANG, W.D., POTET, F., RAI, M., KUPERSHMIDT, S., KNAPIK, E.W., HATZOPOULOS, A.K. 2014. Gremlin 2 promotes differentiation of embryonic stem cells to atrial fate by activation of the JNK signaling pathway. *Stem Cells.,* 32**,** 1774-88.

TIAN, X., HU, T., ZHANG, H., HE, L., HUANG, X., LIU, Q., YU, W., HE, L., YANG, Z., YAN, Y., YANG, X., ZHONG, T.P., PU, W.T., ZHOU, B. 2014. Vessel formation. De novo formation of a distinct coronary vascular population in neonatal heart. *Science. ,* 345**,** 90-94.

TIAN, X., PU, W.T., ZHOU, B. 2015. Cellular origin and developmental program of coronary angiogenesis. *Circ Res.,* 116**,** 515-530.

TOMPERS, D. M., LABOSKY, P.A. 2004. Electroporation of murine embryonic stem cells: a step-by-step guide. *Stem Cells.,* 22**,** 243-9.

TRIEDMAN, J. K., NEWBURGER, J.W. 2016. Trends in Congenital Heart Disease: The Next Decade. *Circulation. ,* 133**,** 2716-33.

TYSER, R. C., MIRANDA, A.M., CHEN, C.M., DAVIDSON, S.M., SRINIVAS, S., RILEY, P.R. 2016. Calcium handling precedes cardiac differentiation to initiate the first heartbeat. *Elife.,* 5.

URNESS, L. D., BLEYL, S.B., WRIGHT ,T.J., MOON, A.M., MANSOUR, S.L. 2011. Redundant and dosage sensitive requirements for Fgf3 and Fgf10 in cardiovascular development. *Dev Biol.,* 356**,** 383-97.

VAN DEN AKKER, N. M., WINKEL, L.C., NISANCIOGLU, M.H., MAAS, S., WISSE, L.J., ARMULIK, A., POELMANN, R.E., LIE-VENEMA, H., BETSHOLTZ, C., GITTENBERGER-DE GROOT, A.C. 2008. PDGF-B signaling is important for murine cardiac development: its role in developing atrioventricular valves, coronaries, and cardiac innervation. *Dev Dyn.,* 237(494-503.

VAN DER LINDE, D., KONINGS, E.E., SLAGER, M.A., WITSENBURG, M., HELBING, W.A., TAKKENBERG, J.J., ROOS-HESSELINK, J.W. 2011. Birth prevalence of congenital heart disease worldwide: a systematic review and meta-analysis. *J Am Coll Cardiol.,* 58**,** 2241-7.

VAN VLIET, P., WU, S.M., ZAFFRAN, S., PUCÉAT, M. 2012. Early cardiac development: a view from stem cells to embryos. *Circ Res.*, 352–362.

VANDUSEN, N. J., CASANOVAS, J., VINCENTZ, J.W., FIRULLI, B.A., OSTERWALDER, M., LOPEZ-RIOS, J., ZELLER, R., ZHOU, B., GREGO-BESSA, J., DE LA POMPA, J.L., SHOU, W., FIRULL, A.B. 2014. Hand2 is an essential regulator for two Notch-dependent functions within the embryonic endocardium. *Cell Rep.,* 9**,** 2071-2083.

VERZI, M. P., MCCULLEY, D.J., DE VAL, S., DODOU, E., BLACK, B.L. 2005. The right ventricle, outflow tract, and ventricular septum comprise a restricted expression domain within the secondary/anterior heart field. *Dev Biol.,* 287**,** 134–145.

VIJAYARAJ, P., LE BRAS, A., MITCHELL, N., KONDO, M., JULIAO, S., WASSERMAN, M., BEELER, D., SPOKES, K., AIRD, W.C., BALDWIN, H.S., OETTGEN, P. 2012. Erg is a crucial regulator of endocardial-mesenchymal transformation during cardiac valve morphogenesis. *Development.,* 139**,** 3973-3985.

WANG, Y., WU, B., CHAMBERLAIN, A.A., LUI, W., KOIRALA, P., SUSZTAK, K., KLEIN, D., TAYLOR, V., ZHOU, B. 2013. Endocardial to myocardial notch-wnt-bmp axis regulates early heart valve development. *PLoS One. ,* 8**,** e60244.

WU, B., WANG, Y., LUI, W., LANGWORTHY, M., TOMPKINS, K.L., HATZOPOULOS, A.K., BALDWIN, H.S., ZHOU, B. 2011. Nfatc1 coordinates valve endocardial cell lineage development required for heart valve formation. *Circ Res.,* 109**,** 183-192.

WU, B., ZHANG, Z., LUI, W., CHEN, X., WANG, Y., CHAMBERLAIN, A.A., MORENO-RODRIGUEZ, R.A., MARKWALD, R.R., O'ROURKE, B.P., SHARP, D.J., ZHENG, D., LENZ, J., BALDWIN, H.S., CHANG, C.P., ZHOU, B. 2012. Endocardial cells form the coronary arteries by angiogenesis through myocardial-endocardial VEGF signaling. *Cell.,* 151():. doi: **,** 1083-1096.

WU, S. M., FUJIWARA, Y., CIBULSKY, S.M., CLAPHAM, D.E., LIEN, C.L., SCHULTHEISS, T.M., ORKIN, S.H. 2006. Developmental origin of a bipotential myocardial and smooth muscle cell precursor in the mammalian heart. *Cell.,* 127**,** 1137-1150.

YUASA, S., ITABASHI, Y., KOSHIMIZU, U., TANAKA, T., SUGIMURA, K., KINOSHITA, M., HATTORI, F., FUKAMI, S., SHIMAZAKI, T., OGAWA, S., OKANO, H., FUKUDA, K. 2005. Transient inhibition of BMP signaling by Noggin induces cardiomyocyte differentiation of mouse embryonic stem cells. *Nat Biotechnol.,* 23**,** 607-11.

ZAFFRAN, S., KELLY, R.G., MEILHAC, S.M., BUCKINGHAM, M.E., BROWN, N.A. 2004. Right ventricular myocardium derives from the anterior heart field. *Circ Res.,* 95**,** 261-268.

ZETTERQVIST, A. V., BERGLUND, L.M., BLANCO, F., GARCIA-VAZ, E., WIGREN, M., DUNÉR, P., ANDERSSON, A.M., TO, F., SPEGEL, P., NILSSON, J., BENGTSSON, E., GOMEZ, MF. 2013. Inhibition of nuclear factor of activated T-cells (NFAT) suppresses accelerated atherosclerosis in diabetic mice. *PLoS One.,* 8**,** e65020. .

ZHANG, H., LUI, K.O., ZHOU, B. 2018. Endocardial Cell Plasticity in Cardiac Development, Diseases and Regeneration. *Circ Res.,* 122**,** 774-789.

ZHANG W, C. H., QU X, CHANG CP, SHOU W. 2013. Molecular mechanism of ventricular trabeculation/compaction and the pathogenesis of the left ventricular noncompaction cardiomyopathy (LVNC). Am J Med Genet C Semin Med Genet*.,* 163C**,** 144-156.

ZHOU, B., WU, B., TOMPKINS, K.L., BOYER, K.L., GRINDLEY, J.C., BALDWIN, H.S. 2005. Characterization of Nfatc1 regulation identifies an enhancer required for gene expression that is specific to pro-valve endocardial cells in the developing heart. *Development.,* 132**,** 1137-1146.